

A realistic model of neutrino masses with a large neutrinoless double beta decay rate

Francisco del Aguila,¹ Alberto Aparici,²

Subhaditya Bhattacharya,³ Arcadi Santamaria,² and Jose Wudka³

¹*CAFPE and Departamento de Fisica Teorica y del Cosmos,*

Universidad de Granada, E-18071 Granada, Spain

²*Departament de Fisica Teorica, Universitat de Valencia and IFIC,*

Universitat de Valencia-CSIC, Dr. Moliner 50,

E-46100 Burjassot (Valencia), Spain

³*Department of Physics and Astronomy,*

University of California, Riverside CA 92521-0413, USA

Abstract

The minimal Standard Model extension with the Weinberg operator does accommodate the observed neutrino masses and mixing, but predicts a neutrinoless double beta ($0\nu\beta\beta$) decay rate proportional to the effective electron neutrino mass, which can be then arbitrarily small within present experimental limits. However, in general $0\nu\beta\beta$ decay can have an independent origin and be near its present experimental bound; whereas neutrino masses are generated radiatively, contributing negligibly to $0\nu\beta\beta$ decay. We provide a realization of this scenario in a simple, well defined and testable model, with potential LHC effects and calculable neutrino masses, whose two-loop expression we derive exactly. We also discuss the connection of this model to others that have appeared in the literature, and remark on the significant differences that result from various choices of quantum number assignments and symmetry assumptions. In this type of models lepton flavor violating rates are also preferred to be relatively large, at the reach of foreseen experiments. Interestingly enough, in our model this stands for a large third mixing angle, $\sin^2 \theta_{13} \gtrsim 0.008$, when $\mu \rightarrow eee$ is required to lie below its present experimental limit.

I. INTRODUCTION

Neutrino oscillations are the only new physics (NP) beyond the minimal Standard Model (SM) observed to date [1] (for recent reviews see for instance [2–4]). They can be fully explained introducing rather small neutrino masses m_ν and the corresponding (unitary) charged current mixing matrix U [5, 6]. The observed pattern of neutrino masses can be implemented, however, in two quite different ways depending on the Dirac or Majorana character of the neutrinos. In the first case the SM is extended by adding three SM singlets, ν_R , to provide Dirac masses to the SM neutrinos, ν_L , through small Yukawa couplings. Alternatively, we can consider extending the SM by adding the only invariant dimension 5 (Weinberg) operator that can be written using the SM field content [7]¹, $\mathcal{O}_5 = \bar{\ell}_L \phi \tilde{\phi}^\dagger \ell_L$. In this case the SM neutrinos acquire Majorana masses after electroweak symmetry breaking, $\langle \phi^0 \rangle = v_\phi$, and are inversely proportional to Λ , the NP scale associated with \mathcal{O}_5 . The small neutrino masses then require that the coefficients of this operator be small, either due to a very large NP scale or suppressed dimensionless couplings.

Both alternatives (that light neutrinos are Dirac or Majorana), are viable and indistinguishable if Λ is very large, *except* for the possible observation of lepton number violation (LNV) in neutrinoless double beta ($0\nu\beta\beta$) decay [8]² (for a recent review see [12]). Indeed, the SM extension with Dirac neutrino masses preserves lepton number (LN), and hence $0\nu\beta\beta$ decay is forbidden. Whereas Majorana masses carry LN equal two, as does the Weinberg operator, and this leads to a non-zero $0\nu\beta\beta$ width. Thus, the observation of $0\nu\beta\beta$ decay would strongly favor Majorana neutrino masses [13]; hence the prime relevance of this type of experiments (see [14, 15] for recent reviews).

All this, however, relies on the assumption that both such minimal SM extensions describe the dominating NP effects up to very high scales. We will argue, however, that LNV and neutrino masses may be due to NP near the electroweak scale, in which case a much richer set of possibilities can be realized. The main point we wish to emphasize is that although both $0\nu\beta\beta$ decay and Majorana neutrino masses do violate LN, they need not be both directly related to the Weinberg operator \mathcal{O}_5 , unlike the above minimal SM extension consisting

¹ ϕ and ℓ_L are the SM Higgs and lepton doublets and $\tilde{\phi} = i\tau_2\phi^*$, $\tilde{\ell}_L = i\tau_2\ell_L^c$.

² We shall not discuss the implications of requiring enough leptogenesis to account for the observed baryogenesis [9] (for recent reviews see [10, 11]).

only of this dimension 5 operator. For instance, the leading LNV effects in $0\nu\beta\beta$ decay could be mediated by an operator involving only *right-handed* (RH) electrons, such as, for example, $\mathcal{O}_9 = (\bar{e}_R e_R^c) \left(\phi^\dagger D^\mu \tilde{\phi} \right) \left(\phi^\dagger D_\mu \tilde{\phi} \right)$ which is the lowest-order LNV operator with two RH leptons and invariant under the SM gauge transformations. In this case \mathcal{O}_5 (with the associated Majorana masses) is generated radiatively by \mathcal{O}_9 at two loops, where the charged leptons suffer a chirality change through mass insertions and are transformed into neutrinos through the exchange of a W boson. This results in a further suppression by two charged lepton masses divided by two powers of the NP mass scale, which we do assume to be close to the electroweak scale. These radiatively-generated Majorana masses will produce the usual contribution to $0\nu\beta\beta$ decay, which, however, will be negligible compared to the \mathcal{O}_9 one.

In a companion paper [16] we classify the different ways of generating $0\nu\beta\beta$ decay and light neutrino masses by the addition of higher order effective operators. This has been studied in the literature [17–20], but mostly for operators involving fermions and scalars; we will concentrate instead on operators involving gauge bosons but not quarks (thus, for example, excluding *ab initio* models with heavy leptoquarks from our analysis). Here we will instead provide a realistic testable model realizing the above scenario, where (i) LN is broken at the electroweak scale; (ii) $0\nu\beta\beta$ decay into two RH electrons has a rate of the order of its experimental limit, through the tree-level exchange of new scalars; and (iii) it contains finite, and therefore calculable, neutrino masses. Despite a relatively small number of parameters this model can also accommodate the observed pattern of neutrino masses and mixings, which are generated at two-loop order (and whose contribution to $0\nu\beta\beta$ decay is in this case negligible). This model is related to others that have been discussed in the literature [21, 22], the differences are crucial, and essential in maintaining the 3 features just mentioned; we discuss these points in detail below.

There are many SM extensions where $0\nu\beta\beta$ decay receive new contributions besides those from light Majorana neutrino masses (see [23] for a general overview). The simplest scenario assumes the presence of heavy Majorana neutrinos whose exchange generates new contributions to $0\nu\beta\beta$ decay, similar to the ones generated by the light neutrinos. (See for recent work [24–27].) Other extensions with many more new particles have also been studied; such as left-right (LR) models [28–30] and supersymmetric extensions (see, for instance, for a review [1], and references there in). In such models there are several contributions to the $0\nu\beta\beta$ decay amplitude, any of which can dominate depending on the region of parameter space

being considered. We are interested, however, in identifying the minimal SM extensions leading to the largest possible contributions to $0\nu\beta\beta$ decay and containing no independent neutrino masses. This means that, as argued above, light neutrino masses only result from the unavoidable contributions mediated by the LNV operators generating $0\nu\beta\beta$ decay; so that the effective Lagrangian approach provides the proper language for classifying such scenarios [16]. Here, we are only concerned with giving a specific example of the case where $0\nu\beta\beta$ and neutrino masses are generated by the same underlying physics but at different orders in perturbation theory, with the former appearing at tree level, while the latter only at two loops³. Simple models with finite neutrino masses at two loops have been often discussed in the literature [32, 33], although not necessarily related to NP inducing $0\nu\beta\beta$ decay as it is the case here.

It is worth emphasizing again that the model we study is one particularly simple example of a class of models realizing the above scenario, and that all such models share many phenomenological implications. In our case the model contains a discrete Z_2 symmetry, which is spontaneously broken. This model has the virtue of providing a direct analysis of the symmetries and scales, however, it also has a domain-wall problem [34, 35]. One way of dealing with this problem is to allow the discrete symmetry to remain unbroken, but at the price of generating both neutrino masses and the $0\nu\beta\beta$ amplitude at a higher loop order; a possibility we will not pursue. We instead discuss related but somewhat more involved models that avoid the domain wall problem while retaining the same low-energy phenomenology. We will restrict ourselves to the most relevant region of parameter space where the $0\nu\beta\beta$ decay rate lies within the reach of the next round of experiments. With this assumption, together with the constraints from lepton flavor violation (LFV) processes such as $\mu \rightarrow eee$, and with the requirement of perturbative unitarity (or if preferred, naturalness of perturbation theory), the model predicts that the neutrino masses obey a normal hierarchy, that the lightest neutrino mass lies in the range $0.002 \text{ eV} \lesssim m_1 \lesssim 0.007 \text{ eV}$, and that the third mixing angle in the Pontecorvo-Maki-Nakagawa-Sakata mixing matrix U [5, 6] obeys $\sin^2 \theta_{13} \gtrsim 0.008$. Value which lies well within the sensitivity of ongoing neutrino oscillation

³ LNV effective operators including quarks also generate neutrino masses but in general at higher loop order, in fact too high in some cases to explain the observed spectrum [31]. Although such operators are not considered in our analysis, we will comment on them further when discussing our general set up in detail [16].

experiments. Besides, the new (charged) scalar masses can be within the LHC reach, and various LFV processes are predicted to have rates that will be probed when present precision is improved by the next generation of experiments.

In next section we present our model; few details on the scalar spectrum and couplings are also worked out, and its relation to other models is briefly discussed. The reader mainly interested in the phenomenological implications of the model can go directly to Section III, where we evaluate the rate for $0\nu\beta\beta$ decay. The requirement that this process can be observed in the next round of experiments, together with perturbativity, translates into upper bounds on the masses of the extra scalars. These, in turn, result in limits on their couplings if present bounds on LFV processes are to be fulfilled, as we show in Section IV. We calculate the neutrino masses in Section V, where we show that the model can accommodate the observed pattern of neutrino masses and mixings, though it predicts a somewhat small electron neutrino effective mass m_{ee} . Finally, the prospects for the discovery of the extra scalars at LHC are considered in Section VI. In connection with this it must be noted that models with extra scalars may allow for a would-be Higgs boson more elusive to LHC searches, for it can have further decay channels open (see for instance [36–38]). Conclusions are drawn in last section. In three Appendices we collect some technical details.

II. A MODEL WITH LEPTON NUMBER SOFTLY BROKEN

This model only extends the SM Higgs sector, in order to allow for scalar couplings to lepton bilinears with non-zero LN. More precisely, as we look for separating the origin of neutrino masses from the mechanism mediating $0\nu\beta\beta$ decay, we only introduce new scalar couplings to RH charged leptons, ensuring they are the only final state produced in tree-level $0\nu\beta\beta$ decay. A simple way to achieve this is to enlarge the Higgs sector including, besides the SM scalar doublet ϕ of hypercharge 1/2, a complex scalar singlet κ of hypercharge 2, a real (neutral) scalar singlet σ , and an electroweak triplet χ of hypercharge 1. We also impose a Z_2 symmetry, under which all SM particles and κ are even while both σ and χ are odd, which forbids their coupling to lepton bilinears. Thus, the Yukawa Lagrangian reads

$$\mathcal{L}_Y = \overline{\ell}_L Y_e e_R \phi + \overline{e}_R^c g e_R \kappa + \text{h.c.} , \quad (1)$$

where we can assume Y_e to be a 3×3 diagonal matrix with positive eigenvalues, and g a complex symmetric matrix with three of its phases unphysical.

The most general Higgs potential consistent with the symmetries is ⁴

$$\begin{aligned}
V = & -m_\phi^2|\phi|^2 - m_\sigma^2\sigma^2 + m_\chi^2\text{Tr}\{\chi^\dagger\chi\} + m_\kappa^2|\kappa|^2 \\
& + \lambda_\phi|\phi|^4 + \lambda_\sigma\sigma^4 + \lambda_\kappa|\kappa|^4 + \lambda_\chi(\text{Tr}\{\chi^\dagger\chi\})^2 + \lambda'_\chi\text{Tr}\{(\chi^\dagger\chi)^2\} \\
& + \lambda_{\phi\sigma}|\phi|^2\sigma^2 + \lambda_{\phi\kappa}|\phi|^2|\kappa|^2 + \lambda_{\phi\chi}|\phi|^2\text{Tr}\{\chi^\dagger\chi\} + \lambda'_{\phi\chi}\phi^\dagger\chi^\dagger\chi\phi \\
& + \lambda_{\sigma\kappa}\sigma^2|\kappa|^2 + \lambda_{\kappa\chi}|\kappa|^2\text{Tr}\{\chi^\dagger\chi\} + \lambda_{\sigma\chi}\sigma^2\text{Tr}\{\chi^\dagger\chi\} \\
& + \left[\mu_\kappa\kappa\text{Tr}\{(\chi^\dagger)^2\} + \lambda_6\sigma\phi^\dagger\chi\tilde{\phi} + \text{h.c.} \right] , \tag{2}
\end{aligned}$$

where by rephasing the fields we can always choose μ_κ and λ_6 real of either sign. For convenience, we will take μ_κ positive and λ_6 negative. In terms of charge eigenstates, the fields χ and ϕ are written

$$\chi = \begin{pmatrix} \chi^+/\sqrt{2} & \chi^{++} \\ \chi^0 & -\chi^+/\sqrt{2} \end{pmatrix}, \quad \phi = \begin{pmatrix} \phi^+ \\ \phi^0 \end{pmatrix}. \tag{3}$$

The singlet σ is introduced to preserve the discrete symmetry that forbids the scalar triplet from coupling to leptons. This symmetry is broken spontaneously by the VEVs $\langle\sigma\rangle$ and $\langle\chi^0\rangle$.

For the phenomenological discussion it is important to note that in the limit of vanishing Y_e , lepton number can be defined to only act on ℓ_L ; this is enough to protect neutrinos from getting a Majorana mass. While the e_R lepton number, which would forbid $0\nu\beta\beta$ decay (into two e_R), is explicitly broken in the scalar potential due to the presence of the μ_κ and λ_6 terms. Therefore, the $0\nu\beta\beta$ decay amplitude will be proportional to all three couplings: g_{ab} in Eq. (1) and μ_κ and λ_6 in Eq.(2); whereas neutrino masses will also depend on Y_e .

This is one of a class of models with the same low energy physics. In order to understand the common LNV features it is convenient to consider the above theory, but with σ complex, and the modifications needed to insure a real Lagrangian. In this case LN is exactly conserved; if leptons are assigned LN -1 , κ carries LN equal to 2, while σ^\dagger and χ both carry LN equal to 1, so that type II see-saw Yukawa couplings $\bar{\ell}_L\chi\ell_L$ are forbidden. The

⁴ Terms like $\text{Tr}\{\chi^2\}\text{Tr}\{\chi^{\dagger 2}\}$, $\text{Tr}\{\chi^2\chi^{\dagger 2}\}$ or $\phi^\dagger\chi\chi^\dagger\phi$ can easily be related to the terms already included by using the fact that for two arbitrary 2×2 traceless matrices $A = A_i\tau_i$ and $B = B_i\tau_i$, $\{A, B\} = \text{Tr}\{AB\}\mathbb{1}$. Other possible terms are forbidden by the discrete symmetry.

vertex $\sigma^\dagger \widetilde{\ell}_L \chi \ell_L$, however, is allowed and generated at two loops, providing light neutrinos a finite mass (which we calculate exactly) after spontaneous symmetry breaking proportional to $\langle \sigma^\dagger \chi \rangle$. Obviously, this model has a Majoron [39] because LN, which is a global abelian symmetry, is spontaneously broken. One can then consider the region of parameter space where such interesting models are phenomenologically viable ⁵, or promote the symmetry to a local one by gauging, for instance, baryon minus lepton number (B–L). Although, this is an interesting possibility, too, with renewed experimental interest (see, for instance, for a review [45]), it requires adding RH neutrinos that provide a new potential source of light neutrino masses; this lies outside the goal of the present investigation that is centered on theories where neutrino masses are generated by the LNV effective operator accounting for $0\nu\beta\beta$ decay.

For this reason we have assumed σ to be real, breaking LN explicitly but leaving as a remnant an exact Z_2 symmetry. The general features of the theory remain, though the Majoron does not appear and LN is reduced to the above Z_2 symmetry ⁶. The spontaneous breaking of this discrete symmetry will generate domain walls. This poses no problem provided $\langle \sigma \rangle$ is sufficiently large (with λ_6 correspondingly small while keeping their product fixed) guaranteeing the formation of such defects before the inflationary epoch. We have assumed instead that $\langle \sigma \rangle$ is not too large because we prefer avoid requiring λ_6 unnaturally small; we may then avoid a domain-wall problem by adding soft-breaking terms, such as σ^3 to the potential (such a modification would not require the introduction of tree-level Yukawa interactions violating the discrete Z_2 symmetry). We do not pursue this discussion because within this class of models there is an even simpler one, with the same neutrino physics at low energy, and none of these potential drawbacks. It is the same model presented above, but with σ replaced by its vacuum expectation value, $\sigma \rightarrow \langle \sigma \rangle$; up to coupling constant redefinition this yields the same potential as Eq. (2) without the terms containing σ , *except*

⁵ In this model the Majoron will be mainly a singlet [39]. In which case its couplings to ordinary matter are small and then little constrained, while its coupling to the Higgs boson is essentially free. Thus, singlet Majorons can result in invisible Higgs decays (see [40] for a recent example). Moreover, they can have interesting implications in astrophysics and cosmology because they can substantially affect the cooling of supernovas [41] and the neutrino relic abundance, due to the possibility of neutrino decaying [42] or annihilating [43] into Majorons. They can be even used as a dark matter candidate (see for instance [44]) if massive (pseudo-Majorons).

⁶ One can also assign an odd Z_2 parity to the leptons, in which case this discrete symmetry equals $(-1)^{LN}$.

for the last term that becomes $\mu_\chi \phi^\dagger \chi \tilde{\phi}$, with

$$\mu_\chi = \lambda_6 \langle \sigma \rangle , \quad (4)$$

of the order of a TeV. Obviously, the resulting renormalizable Lagrangian has the same quantum behaviour than ours; in particular, neutrino masses are finite and generated at two loop order and can be obtained from our results by eliminating λ_6 using (4). We will prefer to discuss the model including the real scalar field σ because the perturbative and symmetry analyses appear to be more transparent to us. In the minimal model with the SM addition of only κ and χ , and the scalar potential terms relating their LN charges $\mu_\kappa \kappa \text{Tr} \left\{ (\chi^\dagger)^2 \right\}$ and $\mu_\chi \phi^\dagger \chi \tilde{\phi}$ the LN of the χ field is not well defined since the first term requires it to be 1 while the second 0 (though never 2); as a consequence the effective vertex $Y_\chi \overline{\ell}_L \chi \ell_L$, is finite and generated radiatively ⁷. Despite the parallels of this discussion with models implementing a type II see-saw mechanism (which contain a tree-level $\overline{\ell}_L \chi \ell_L$ coupling) there is an important difference, namely, that in such theories both the expression for the neutrino masses and the $0\nu\beta\beta$ decay amplitude are *linear* in $\langle \chi \rangle$; in contrast the corresponding results in our model are proportional to $\langle \chi \rangle^2$ (see Eqs. (25) and (33) below).

The extension of the SM model we consider is related to the one presented in Refs. [21, 22] as far as particle content is concerned (we differ by adding the singlet σ). However, the symmetries and quantum number assignments are different, which proves a crucial difference. Had we included the hard term $\kappa \phi^\dagger \chi^\dagger \tilde{\phi}$ as was done in the above references, χ should have been assigned LN = 2; this would necessitate also including the tree-level coupling $\overline{\ell}_L \chi \ell_L$ that would lead to the usual type II see-saw scenario. In particular it would have been inconsistent to assign LN zero to χ or to arbitrarily exclude this Yukawa coupling from the Lagrangian, for its coefficient would receive divergent radiative corrections; in consequence the neutrino masses are not calculable. If one requires χ to have LN equal to 0, as was done in these publications, the quartic coupling $\kappa \phi^\dagger \chi^\dagger \tilde{\phi}$ must be absent; but then LN remains unbroken and the light neutrino masses must vanish to all orders which is again inconsistent with the results presented there.

⁷ Note that in the theory containing an extra real scalar σ , one could also reason differently to justify this result. Indeed, we could assign σ LN equal to 0; then the quartic term $\sigma \phi^\dagger \chi \tilde{\phi}$ fixes the χ LN also equal to 0, while the trilinear term $\kappa \text{Tr}\{(\chi^\dagger)^2\}$ breaks LN softly. In any case the discrete Z_2 symmetry guarantees that the neutrino masses stay finite.

A. The scalar spectrum

The requirement on the scalar potential of being bounded from below is fulfilled restricting the quartic couplings in Eq. (2) adequately; these conditions include ⁸

$$\lambda_\sigma, \lambda_\phi > 0, \quad \lambda_{\phi\sigma} > -2\sqrt{\lambda_\sigma\lambda_\phi}. \quad (5)$$

We have also checked that there is a non-trivial minimum on which the scalar neutral components acquire non-zero expectation values: $v_\phi \equiv \langle \phi^0 \rangle > 0$, $v_\chi \equiv \langle \chi^0 \rangle > 0$, $v_\sigma \equiv \langle \sigma \rangle > 0$, with

$$\phi^0 = \langle \phi^0 \rangle + \frac{1}{\sqrt{2}}(\phi_R + i\phi_I), \quad \chi^0 = \langle \chi^0 \rangle + \frac{1}{\sqrt{2}}(\chi_R + i\chi_I), \quad \sigma = \langle \sigma \rangle + \sigma_R. \quad (6)$$

In Appendix A we comment on the experimental limit on the scalar triplet VEV v_χ , which we will find to be of the order of few GeV; to be conservative we will assume $v_\chi < 5$ GeV, this satisfies $v_\chi \ll v_\phi \approx 174$ GeV where $1/(v_\phi^2 + 2v_\chi^2) = g^2/2m_W^2 = 2\sqrt{2}G_F$ (derived from Eq. (A2) and the experimental limit on the ρ parameter, $|\rho_0 - 1| \ll 1$ [1]). In this approximation the minimization conditions can be easily solved:

$$v_\chi \approx \frac{-\lambda_6 v_\sigma v_\phi^2}{m_\chi^2 + v_\phi^2 \lambda_{\phi\chi} + v_\sigma^2 \lambda_{\sigma\chi}}, \quad v_\phi^2 \approx \frac{2\lambda_\sigma m_\phi^2 - \lambda_{\phi\sigma} m_\sigma^2}{4\lambda_\sigma \lambda_\phi - \lambda_{\phi\sigma}^2}, \quad v_\sigma^2 \approx \frac{2\lambda_\phi m_\sigma^2 - \lambda_{\phi\sigma} m_\phi^2}{4\lambda_\sigma \lambda_\phi - \lambda_{\phi\sigma}^2}. \quad (7)$$

Notice that the phase choice $\lambda_6 < 0$ is consistent with v_χ being real and positive. We set the σ and ϕ mass squared terms in the Higgs potential negative to favour the development of such a minimum. Though we choose the χ mass squared term positive, this field also acquires a small VEV induced by the doublet and singlet VEVs, similar to the case observed in see-saw of type II models [46–48].

The scalar masses can be obtained by substituting Eq. (6) in the potential. Using the exact minimization conditions to eliminate m_ϕ and m_σ in favour of the VEVs, the mass

⁸ Notice that the term $|\phi|^2\sigma^2$ is always positive.

terms for the charged scalars can be written

$$\mathcal{L}_M = -(\kappa^{--} \ \chi^{--}) M_D^2 \begin{pmatrix} \kappa^{++} \\ \chi^{++} \end{pmatrix} - (\phi^- \ \chi^-) M_S^2 \begin{pmatrix} \phi^+ \\ \chi^+ \end{pmatrix}, \text{ with} \quad (8)$$

$$M_D^2 = \begin{pmatrix} m_\kappa^2 + v_\phi^2 \lambda_{\phi\kappa} + v_\sigma^2 \lambda_{\sigma\kappa} + v_\chi^2 \lambda_{\kappa\chi} & 2\mu_\kappa v_\chi \\ 2\mu_\kappa v_\chi & m_\chi^2 + v_\phi^2 (\lambda_{\phi\chi} + \lambda'_{\phi\chi}) + v_\sigma^2 \lambda_{\sigma\chi} + 2v_\chi^2 \lambda'_{\chi} \end{pmatrix}, \quad (9)$$

$$M_S^2 = \frac{(v_\chi \lambda'_{\phi\chi} - 2v_\sigma \lambda_6)}{2v_\chi} \begin{pmatrix} 2v_\chi^2 & -\sqrt{2}v_\phi v_\chi \\ -\sqrt{2}v_\phi v_\chi & v_\phi^2 \end{pmatrix}. \quad (10)$$

Analogously for the neutral sector

$$\mathcal{L}_M = -\frac{1}{2}(\phi_I \ \chi_I) M_I^2 \begin{pmatrix} \phi_I \\ \chi_I \end{pmatrix} - \frac{1}{2}(\phi_R \ \chi_R \ \sigma_R) M_R^2 \begin{pmatrix} \phi_R \\ \chi_R \\ \sigma_R \end{pmatrix}, \text{ with} \quad (11)$$

$$M_I^2 = -\frac{v_\sigma \lambda_6}{v_\chi} \begin{pmatrix} 4v_\chi^2 & -2v_\phi v_\chi \\ -2v_\phi v_\chi & v_\phi^2 \end{pmatrix}, \quad (12)$$

$$M_R^2 = \begin{pmatrix} 4v_\phi^2 \lambda_\phi & 2v_\phi (v_\sigma \lambda_6 + v_\chi \lambda_{\phi\chi}) & 2\sqrt{2}v_\phi (v_\sigma \lambda_{\phi\sigma} + v_\chi \lambda_6) \\ 2v_\phi (v_\sigma \lambda_6 + v_\chi \lambda_{\phi\chi}) & 4v_\chi^2 (\lambda_\chi + \lambda'_\chi) - v_\phi^2 v_\sigma \lambda_6 / v_\chi & \sqrt{2} (v_\phi^2 \lambda_6 + 2v_\sigma v_\chi \lambda_{\sigma\chi}) \\ 2\sqrt{2}v_\phi (v_\sigma \lambda_{\phi\sigma} + v_\chi \lambda_6) & \sqrt{2} (v_\phi^2 \lambda_6 + 2v_\sigma v_\chi \lambda_{\sigma\chi}) & 8v_\sigma^2 \lambda_\sigma - 2v_\phi^2 v_\chi \lambda_6 / v_\sigma \end{pmatrix} \quad (13)$$

All eigenvalues of these mass matrices must be positive (except for the would-be Goldstone bosons providing the longitudinal vector boson degrees of freedom) in order to guarantee that the solution to the minimization conditions corresponds to a local minimum. This sets further constraints on the model parameters, which can be satisfied rather easily, especially in the limit $m_\chi \gg v_{\phi,\sigma,\chi}$.

Thus, we are left with two massive doubly-charged scalars $\kappa_{1,2}$,

$$\begin{aligned} \kappa_1 &= \cos \theta_D \kappa^{++} + \sin \theta_D \chi^{++}, \\ \kappa_2 &= -\sin \theta_D \kappa^{++} + \cos \theta_D \chi^{++}, \end{aligned} \quad (14)$$

with

$$\sin 2\theta_D = 2 \sin \theta_D \cos \theta_D = \frac{4\mu_\kappa v_\chi}{m_{\kappa_1}^2 - m_{\kappa_2}^2}, \quad (15)$$

and only one massive, mainly triplet, singly-charged scalar ω ,

$$\omega^+ = -\sin \theta_S \phi^+ + \cos \theta_S \chi^+, \text{ with } \tan \theta_S = \frac{\sqrt{2}v_\chi}{v_\phi}. \quad (16)$$

Similarly, there is a neutral scalar A with imaginary components,

$$A = -\sin\theta_I\phi_I + \cos\theta_I\chi_I \quad , \quad \text{with} \quad \tan\theta_I = \frac{2v_\chi}{v_\phi} \quad . \quad (17)$$

There are also three neutral scalars along the real components ϕ_R , χ_R , σ_R . We will denote these mass eigenfields by h (mainly doublet), H (mainly triplet) and s (mainly singlet). They are obtained rotating the current fields, what introduces other three mixing angles. Notice that in the limit $m_\chi \gg v_{\phi,\sigma}$, we have $v_\chi \ll v_{\phi,\sigma}$ and $m_{\kappa_2,\omega,A} \approx m_\chi$, with all mixings small.

B. Some scalar couplings of phenomenological interest

Once the quadratic terms of the Lagrangian are diagonalized we can read the interactions for the mass eigenfields. In the following we will need the scalar coupling to RH electrons

$$\overline{e_{Ra}^c} g_{ab} e_{Rb} (\cos\theta_D\kappa_1 - \sin\theta_D\kappa_2) + \text{h.c.} \quad , \quad (18)$$

and the corresponding doubly-charged scalar couplings to gauge bosons

$$g^2\chi^{0\dagger}W_\mu^-W^{\mu-}\chi^{++} + \text{h.c.} \rightarrow g^2v_\chi W_\mu^-W^{\mu-}(\sin\theta_D\kappa_1 + \cos\theta_D\kappa_2) + \text{h.c.} \quad , \quad (19)$$

as well as their trilinear couplings

$$-\mu_\kappa\kappa^{++}(\chi^-)^2 - 2\mu_\kappa\kappa^{++}\chi^{--}\chi^{0\dagger} + \lambda_6\sigma(\phi^-)^2\chi^{++} + \text{h.c.} \quad , \quad (20)$$

which can be also expressed in terms of the mass eigenfields using Eqs. (14–16), and the corresponding VEVs in Eq. (6). Finally, the Yukawa coupling changing charge and chirality writes

$$\overline{\nu_L} Y_e e_R \phi^+ + \text{h.c.} = \overline{\nu_L} Y_e e_R (\cos\theta_S G^+ - \sin\theta_S \omega^+) + \text{h.c.} \quad , \quad (21)$$

where $G^+ = \cos\theta_S\phi^+ + \sin\theta_S\chi^+$ is the would-be Goldstone boson providing the third component to the W .

III. NEUTRINOLESS DOUBLE BETA DECAY

Both doubly-charged scalars $\kappa_{1,2}$ have components along the singlet κ^{++} and the triplet χ^{++} . Therefore, they (respectively) contain couplings to RH electrons and to W 's, generating an effective vertex $eeWW$ that mediates $0\nu\beta\beta$ decay. In this section we calculate

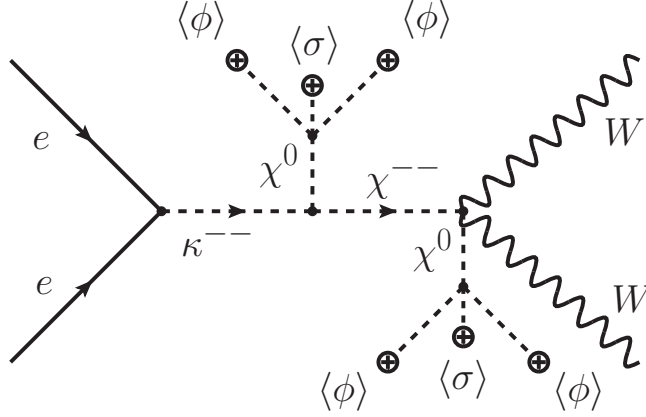


Figure 1: Dominant tree-level diagram contributing to the effective neutrinoless double beta decay operator.

this contribution to $0\nu\beta\beta$ decay and obtain the explicit constraints on the model parameters derived from the assumption that $0\nu\beta\beta$ decay will be observed in the next round of experiments.

Assuming that $m_{\kappa,\chi} \gg v_{\phi,\sigma}$ and integrating out the heavy κ and χ modes we find, after a straightforward calculation, that the effective Lagrangian contains the term

$$\mathcal{L}_9 = \frac{4(\lambda_6 v_\sigma)^2 \mu_\kappa}{m_\kappa^2 m_\chi^6} (\bar{e}_{Ra} g_{ab}^* e_{Rb}^c) \left(\phi^\dagger D^\mu \tilde{\phi} \right) \left(\phi^\dagger D_\mu \tilde{\phi} \right) + \text{h.c.} , \quad (22)$$

as announced in the Introduction, and discussed in the companion paper [16]. One can better understand the origin of this LNV interaction by considering the contribution of the dominant diagram in Fig. 1, where the different couplings and VEVs involved are displayed explicitly. The corresponding $eeWW$ vertex at low energy ($q^2 \ll m_{\kappa_{1,2}}^2$) can be written as ⁹

$$\mathcal{L}_{eeWW} = -\frac{2g^2 \mu_\kappa v_\chi^2}{m_{\kappa_1}^2 m_{\kappa_2}^2} e_{Ra} g_{ab}^* e_{Rb}^c W^\mu W_\mu + \text{h.c.} , \quad (23)$$

where we have summed up all possible mass insertions in the internal propagator, and used Eq. (15). This expression coincides with Eq. (22) when the scalar doublets develop a VEV in the limit of large $m_{\kappa,\chi} (\gg v_{\phi,\sigma})$, *i.e.*, $v_\chi \approx -\lambda_6 v_\sigma v_\phi^2 / m_\chi^2$ and $m_\kappa \approx m_{\kappa_1}$, $m_\chi \approx m_{\kappa_2}$.

Let us particularize to the case $a = b = e$, relevant for $0\nu\beta\beta$, and further integrate the

⁹ It must be emphasized that the Lagrangian violating LN by 2 units for $0\nu\beta\beta$ decay is proportional to v_χ^2 . This must be compared with the linear dependence in v_χ obtained when the χ LN assignment is 2.

two W 's to obtain the appropriate 6-fermion contact interaction

$$\mathcal{L}_{0\nu\beta\beta} = \frac{G_F^2}{2m_p} \epsilon_3 (\bar{u}\gamma^\mu(1 - \gamma_5)d) (\bar{u}\gamma_\mu(1 - \gamma_5)d) \bar{e}(1 - \gamma_5)e^c, \quad (24)$$

where m_p denotes the proton mass and

$$\epsilon_3 = -\frac{8m_p\mu_\kappa v_\chi^2}{m_{\kappa_1}^2 m_{\kappa_2}^2} g_{ee}^*. \quad (25)$$

This type of interactions has been already considered in the literature [49], where limits from the most sensitive experiments at that moment were derived. Since they have not been substantially improved, we will directly use the results in [49] from the Heidelberg-Moscow experiment corresponding to $T_{1/2} > 1.9 \times 10^{25}$ years which yields ¹⁰ $\epsilon_3 < 1.4 \times 10^{-8}$ at 90% C.L. On the other hand, experiments in the near future will be sensitive to lifetimes of the order of 6×10^{27} years [14], *i.e.* a reduction factor on the coupling of roughly 0.05. Then, in order to $0\nu\beta\beta$ decay be observable in the next round of experiments but still satisfy the present limits, we must require

$$8.75 \times 10^{-11} \overset{\text{Next}}{<} \frac{m_p\mu_\kappa v_\chi^2}{m_{\kappa_1}^2 m_{\kappa_2}^2} |g_{ee}| < 1.75 \times 10^{-9} \quad (90\% \text{ C.L.}), \quad (26)$$

where m_p is the proton mass and the inequality with the superscript "Next" corresponds to the requirement that $0\nu\beta\beta$ decay will be observed in the next generation of experiments [14]. While the inequality without the superscript stands for the present experimental limit at the 90% C.L.. The conditions in Eq. (26) will prove rather restrictive because its range of variation is relatively narrow. In fact, reducing the lower limit will appreciable enlarge the allowed parameter region as discussed below.

Thus, the above lower limit together with the requirement of perturbative unitarity (indicated by the "Pert" superscript in the inequalities below) or naturalness, which bounds from above the product of couplings and VEVs $\mu_\kappa v_\chi^2 |g_{ee}|$, translate into an upper limit on the product of the scalar masses $m_{\kappa_{1,2}}$. These, however, are not precisely established because the perturbative bounds are in fact estimates that vary with the approach. In Fig. 2 we show the allowed $m_\kappa - m_\chi$ region, where $m_\kappa \approx m_{\kappa_1}$ and $m_\chi \approx m_{\kappa_2}$ in the limit of small mixing angle θ_D , for $v_\chi = 2$ (blue, darker) and 5 (orange, lighter) GeV (see Appendix A),

¹⁰ There is a misprint in Ref. [49]. We thank the authors of this reference for providing us with the correct limit on ϵ_3 .

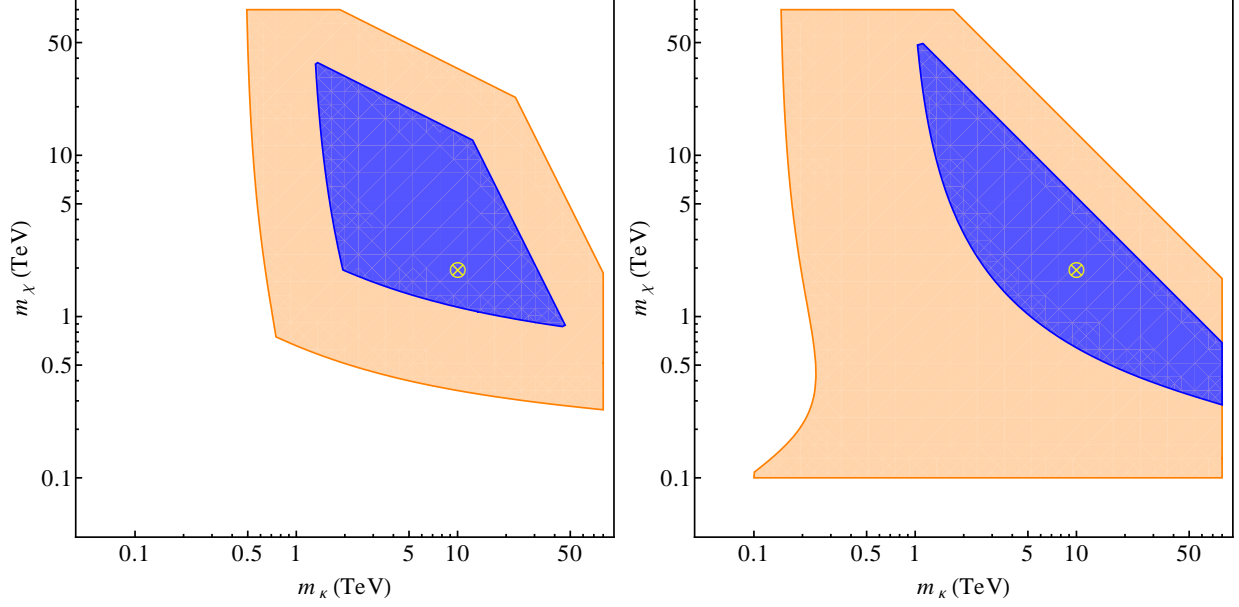


Figure 2: Projection on the $m_\kappa - m_\chi$ plane of the allowed parameter space region, with $m_\kappa \approx m_{\kappa_1}$ and $m_\chi \approx m_{\kappa_2}$. On the left (right) we draw the region assuming perturbative unitarity (a LN breaking scale $\mu_\kappa < 20$ TeV). The blue, darker (orange, lighter) areas correspond to $v_\chi = 2$ (5) GeV. The crosses stand for the reference point $m_{\kappa_1} = 10$ TeV, $m_{\kappa_2} = 2$ TeV (and $v_\chi = 2$ GeV, $\mu_\kappa = 15$ TeV, with $g_{ee} = 1$ and $g_{e\mu} = 0.001$).

respectively, assuming perturbative unitarity (left) and a maximum LN breaking scale μ_κ (right). In the first case (see Eqs. (B1) and (B2) in Appendix B)

$$|g_{ee}|^{\text{Pert}} < \sqrt{4\pi}, \quad \mu_\kappa^{\text{Pert}} < 4\pi \min(m_{\kappa_{1,2}}); \quad (27)$$

whereas in the second one

$$|g_{ee}|^{\text{Pert}} < \sqrt{4\pi}, \quad \mu_\kappa < 20 \text{ TeV}. \quad (28)$$

It must be noticed that all (pseudo-)observables violating LN are proportional to $\mu_\kappa v_\chi^2$. Hence, an increase in v_χ can be traded by the corresponding increase in μ_κ , and vice-versa. So, the orange areas in Fig. 2 can be also interpreted as the allowed regions for $v_\chi = 2$ GeV and $\mu_\kappa^{\text{Pert}} < 25\pi \min(m_{\kappa_{1,2}})$ (left) and $\mu_\kappa < 125$ TeV (right). One may wonder at this point why we choose the bound of 20 TeV for μ_κ in Eq. (28); or equivalently, what is the effect of varying such a value. The answer is simple. The blue, darker region in the right panel of Fig. 2 disappears for $\mu_\kappa \lesssim 8$ TeV, which only reflects the narrowness of the range allowed

by Eq. (26), as required by our main working assumption that $0\nu\beta\beta$ decay will be observed in the next round of experiments. The allowed regions in Fig. 2 are appreciably enlarged by reducing the lower limit in this equation. This can also be achieved by further increasing μ_κ .

These areas are also bounded from below due to the non-observation of doubly-charged scalars; we can then assume $m_{\kappa_{1,2}} > 100$ GeV, as discussed in Section VI. However, the enclosed areas in Fig. 2 are further reduced by a more stringent and subtle constraint. As we shall discuss below, bounds on LFV processes (see section IV) like $\tau^- \rightarrow e^+\mu^-\mu^-$ banish m_κ to large values if the corresponding coupling product $g_{\tau e}g_{\mu\mu}^*$ is sizeable, which is required because neutrino masses are proportional to g_{ab} (see section V), and $g_{\tau e}$ and $g_{\mu\mu}$ must be large in order to accommodate the observed neutrino spectrum. Moreover, both m_κ and m_χ enter in the two-loop integrals generating neutrino masses, but these tend to zero in the limit $m_\chi/m_\kappa \rightarrow 0$. As a result, both scalar masses are constrained, but differently, by the $\tau^- \rightarrow e^+\mu^-\mu^-$ bound. The regions in Fig. 2 satisfy all experimental restrictions, including the upper bound in Eq. (26). The LHC will further reduce the allowed regions, mainly in the case of large LN breaking scale μ_κ . We also provide a ‘‘benchmark point’’, denoted by a cross in the figures, where all constraints are satisfied, and which we will use as reference throughout the paper. As can be deduced from this Figure the parameter space is rather constrained in this simple model when we require that the values of couplings and scalar masses stay natural, but one can think of other models within this class of theories where these constraints are significantly relaxed (at the price of complicating the spectrum through the introduction of additional scalars).

IV. LEPTON FLAVOR VIOLATION CONSTRAINTS

We will show in the next section that in order to obtain neutrino masses in agreement with experiment, the doubly-charged scalar Yukawa couplings g_{ab} and the m_χ/m_κ ratio cannot be too small. In such a case some of the predicted LFV rates can become large enough to be at the verge of their present experimental bounds, especially for very rare processes like $\mu^- \rightarrow e^+e^-e^-$ or $\mu^- \rightarrow e^-\gamma$. Thus, we can use LFV processes to further constrain the model, and perhaps to confirm or exclude it in the near future.

In this section we will briefly discuss the most restrictive process $\mu^- \rightarrow e^+e^-e^-$, whose

tree-level amplitude is obtained by the single exchange of the doubly-charged scalar κ . The corresponding branching ratio equals

$$\text{BR}(\ell_a^- \rightarrow \ell_b^+ \ell_c^- \ell_d^-) = \frac{1}{2(1 + \delta_{cd})} \left| \frac{g_{ab} g_{cd}^*}{G_F \tilde{m}_\kappa^2} \right|^2 \text{BR}(\ell_a^- \rightarrow \ell_b^- \nu \bar{\nu}), \quad (29)$$

where δ_{cd} takes into account the fact that there may be two identical particles in the final state, as in our case, and

$$\frac{1}{\tilde{m}_\kappa^2} \equiv \frac{\cos^2 \theta_D}{m_{\kappa_1}^2} + \frac{\sin^2 \theta_D}{m_{\kappa_2}^2}. \quad (30)$$

(If $\sin^2 \theta_D \ll 1$, the effective mass $\tilde{m}_\kappa \approx m_{\kappa_1}$ since we, in practice, assume that $m_{\kappa_{1,2}}$ are never very different.) Then, the current experimental limit on $\text{BR}(\mu^- \rightarrow e^+ e^- e^-) < 1.0 \times 10^{-12}$ [1] translates into

$$|g_{\mu e} g_{ee}^*| < 2.3 \times 10^{-5} (\tilde{m}_\kappa / \text{TeV})^2, \quad (31)$$

which is mainly a constraint on $g_{\mu e}$ because g_{ee} must be relatively large if $0\nu\beta\beta$ decay has to be observable at the next generation of experiments.

Related processes provide weaker constraints. Thus, $\mu^- \rightarrow e^- \gamma$ proceeds at one loop and is suppressed by the corresponding loop factor, and similarly for $\mu - e$ conversion in nuclei. The bounds from $\mu^+ e^- \longleftrightarrow \mu^- e^+$ (muonium-antimuonium conversion) or muon-positron conversion, although tree-level processes, are also less restrictive (for a discussion of LFV processes mediated by doubly-charged scalar singlets in a similar model see [50, 51]). All these processes and the analogous ones involving τ leptons, as well as the corresponding (anomalous) magnetic moments will be discussed in detail with more generality elsewhere.

Here we shall be mainly interested in the interplay of a large $0\nu\beta\beta$ decay rate and a realistic pattern of Majorana masses, and for this purpose it is sufficient to show the restrictions on these (pseudo-)observables in simple SM extensions as the one at hand, and indicate which further processes may be within the reach of new experiments. In our case, the most restrictive process besides $\mu^- \rightarrow e^+ e^- e^-$ is $\tau^- \rightarrow e^+ \mu^- \mu^-$, which will be discussed below taking into account the neutrino mass requirements.

V. NEUTRINO MASS GENERATION AND θ_{13} EXPECTATION

In the model under consideration LN is not conserved when the couplings μ_κ , λ_6 , g_{ab} and Y_e are non-vanishing. In this case there is no protection against the neutrinos acquiring

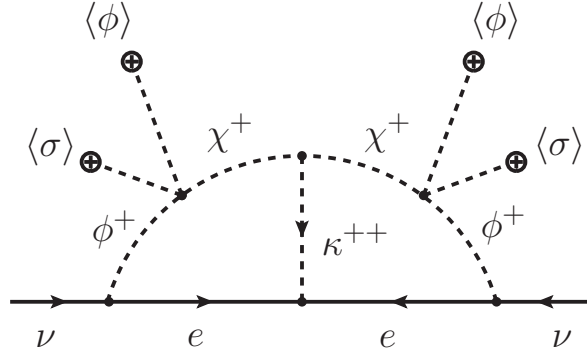


Figure 3: Two-loop diagram contributing to neutrino masses.

Majorana masses m_ν , which will then be proportional to all four couplings, are finite, and appear at the two-loop level, as explained in Section II and shown by explicit calculation in Appendix C. (If any of these couplings vanishes a conserved lepton number remains after spontaneous symmetry breaking and the neutrino masses will vanish.) These masses are generated by the non-renormalizable interaction $\sigma \bar{\ell}_L \chi \ell_L$ generated at two loops, when σ and χ develop VEVs; the corresponding coupling being $m_\nu/v_\sigma v_\chi$. In contrast, the see-saw type II coupling $\bar{\ell}_L \chi \ell_L$ violates the Z_2 symmetry and is forbidden to all orders.

In Fig. 3 we draw one of the diagrams. Defining the neutrino mass matrix as usual,

$$\mathcal{L}_m = -\frac{1}{2} \bar{\nu}_L m_\nu \nu_L^c + \text{h.c.} , \quad (32)$$

we can write, taking $v_\chi \ll v_\phi$ (see Eq. (A3) and Appendix A),

$$(m_\nu)_{ab} = \frac{\mu_\kappa v_\chi^2}{2(2\pi)^4 v_\phi^4} m_a g_{ab}^* m_b I_\nu , \quad (33)$$

where I_ν is the sum of the (rescaled) loop integrals from the different graphs¹¹. I_ν can be estimated in the mass insertion approximation with $m_{\kappa,\chi} \gg m_W$. For instance, in this limit one of the contributions, I_1 , corresponding to the diagram in Fig. 3 gives (neglecting the lepton masses in the denominator and assuming equal masses for the doubly and singly-charged triplet components)

$$I_1 = (4\pi)^4 m_\chi^4 \int \frac{k \cdot q}{k^4 (k^2 - m_\chi^2) q^4 (q^2 - m_\chi^2) ((k - q)^2 - m_\kappa^2)} . \quad (34)$$

¹¹ Again we note that neutrino masses, which violate LN by 2 units, are proportional to v_χ^2 in our case. In contrast the dependence is linear in the estimate for the model in Refs. [21, 22], showing that χ must be assigned LN 2, as in see-saw models of type II. Besides, the neutrino masses are in fact infinite in that particular case, a point obscured because divergent diagrams were omitted.

In this approximation the full I_ν is a dimensionless function of $y = (m_\chi/m_\kappa)^2$ of order one, except for $y \rightarrow 0$, in which case it tends to zero as $y \log y$. In contrast with I_1 which tends faster to zero, as $(y \log y)^2$, for vanishing y . I_ν is also bounded from above, going to a constant of order 2 for $y \rightarrow \infty$. A complete calculation taking into account the W -mass, as well as the v_χ corrections and the new scalar mass scales, is presented in Appendix C. A reasonable approximation is to neglect higher v_χ effects and take all triplet masses equal $m_{\kappa_2} = m_\omega = m_A$; in fact, in the physical limit $v_\chi \ll v_\phi$, κ_2 is mainly the doubly-charged triplet component, ω the singly-charged one, and A the imaginary part of the neutral triplet component.

In our model the Yukawa couplings g_{ab} appear in the neutrino mass matrix, the $0\nu\beta\beta$ decay amplitude and the amplitudes for the LFV processes, and this translates into rather stringent constraints on the allowed neutrino mass matrices (once one insists in dealing with a perturbative theory up to several tens of TeV). We now consider these constraints.

Assuming $\mu_\kappa \sim 10$ TeV and $v_\chi < 2$ GeV, and taking $I_\nu, |g_{ee}| \sim 1$, Eq. (33) gives $|(m_\nu)_{ee}| \sim 3.7 \times 10^{-6}$ eV. How large can it be in general? Using perturbativity limits (27) and $I_\nu \sim 1$, we get

$$|(m_\nu)_{ee}| \stackrel{\text{Pert}}{<} 1.6 \times 10^{-5} \left(\frac{\min(m_{\kappa_{1,2}})}{\text{TeV}} \right) \text{eV} \stackrel{\text{Next,Pert}}{<} 1.6 \times 10^{-4} \text{eV}, \quad (35)$$

where the upper limit is obtained by taking $\min(m_{\kappa_{1,2}}) \sim 10$ TeV (see Fig. 2, left). Alternatively, we can translate the limits on $0\nu\beta\beta$ decay in Eq. (26) into bounds on $(m_\nu)_{ee}$, but for large scalar masses this limit is less stringent than (35). In either case, $|(m_\nu)_{ee}|$ is typically less than 10^{-4} .

There is in addition a quite strong bound on $(m_\nu)_{e\mu}$ from $\mu \rightarrow eee$. Substituting Eq. (31) in the generic neutrino mass expression in Eq. (33) we find

$$|(m_\nu)_{e\mu}| < 2.3 \times 10^{-5} \left(\frac{\tilde{m}_\kappa}{\text{TeV}} \right)^2 \frac{\mu_\kappa v_\chi^2}{2(2\pi)^4 v_\phi^4} \frac{m_e m_\mu}{|g_{ee}|} I_\nu. \quad (36)$$

The constraint that a signal is seen in near-future $0\nu\beta\beta$ decay experiments (left inequality in Eq. (26)) can then be used to eliminate $|g_{ee}|$; in this way we obtain

$$|(m_\nu)_{e\mu}| \stackrel{\text{Next}}{<} 4.3 I_\nu \frac{\tilde{m}_\kappa^2 \mu_\kappa^2}{m_{\kappa_1}^2 m_{\kappa_2}^2} \frac{v_\chi^4}{v_\phi^4} \text{eV} \stackrel{\text{Next,Pert}}{<} 1.2 \times 10^{-5} \text{eV}, \quad (37)$$

where in the second inequality we used $I_\nu \sim 1$, $v_\chi = 2$ GeV, the naturality limit on μ_κ (Eq. (27)), and $\sin \theta_D \ll 1$. If we had used the LN breaking scale $\mu_\kappa = 10$ TeV and the production limit on $m_{\kappa_2} > 0.1$ TeV, then $|(m_\nu)_{e\mu}| < 7 \times 10^{-4}$.

The final result of this phenomenological discussion is that both, $|(m_\nu)_{ee}|$ and $|(m_\nu)_{e\mu}|$, must be below $\sim 10^{-4}$ eV, and this follows from requiring that (i) $0\nu\beta\beta$ decay is at the reach of the next round of experiments, and (ii) that the theory is perturbative and free of unnatural fine tuning up to several tens of TeV. These limits could be somewhat relaxed: in the $|(m_\nu)_{ee}|$ case by making doubly-charged scalar masses larger, and in the $|(m_\nu)_{e\mu}|$ case by allowing for a smaller $|g_{ee}|$. However, this is at the price of generating some tension with the naturalness constraint in the former case, and spoiling the possibility of observing $0\nu\beta\beta$ decay induced by scalars in the near future in the latter one. There are additional but less severe bounds on the remaining g_{ab} from other LFV processes; we discuss them below, when presenting the plots for the relevant neutrino mass (pseudo-)observables satisfying present experimental restrictions.

A. Prediction for the third neutrino mixing angle θ_{13}

The question now becomes whether it is possible to accommodate the observed spectrum of neutrino masses and mixing angles in this type of models once the above experimental constraints are imposed. In the following we will use the standard parameterization of the neutrino mass matrix [1, 48, 52, 53] in terms of 3 mass parameters, 3 mixing angles and 3 phases:

$$m_\nu = UD_\nu U^T, \quad \text{with } D_\nu = \text{diag}(m_1, m_2, m_3) \quad (38)$$

and

$$U = \begin{pmatrix} c_{13}c_{12} & c_{13}s_{12} & s_{13}e^{-i\delta} \\ -c_{23}s_{12} - s_{23}s_{13}c_{12}e^{i\delta} & c_{23}c_{12} - s_{23}s_{13}s_{12}e^{i\delta} & s_{23}c_{13} \\ s_{23}s_{12} - c_{23}s_{13}c_{12}e^{i\delta} & -s_{23}c_{12} - c_{23}s_{13}s_{12}e^{i\delta} & c_{23}c_{13} \end{pmatrix} \begin{pmatrix} e^{i\alpha_1/2} \\ e^{i\alpha_2/2} \\ 1 \end{pmatrix}, \quad (39)$$

where $s_{ij} \equiv \sin \theta_{ij}$ and $c_{ij} \equiv \cos \theta_{ij}$. A global fit to neutrino oscillation data gives (see, for instance, [54]) $\Delta m_{21}^2 \equiv m_2^2 - m_1^2 = (7.59_{-0.18}^{+0.20}) \times 10^{-5} \text{ eV}^2$, $\Delta m_{31}^2 \equiv m_3^2 - m_1^2 = (2.50_{-0.16}^{+0.09}) \times 10^{-3} \text{ eV}^2$, $s_{12}^2 = 0.312_{-0.015}^{+0.017}$, $s_{23}^2 = 0.52_{-0.07}^{+0.06}$, $s_{13}^2 = 0.013_{-0.005}^{+0.007}$. Neutrino oscillations are not sensitive to the phases α_1 and α_2 , nor to a common mass scale which is conventionally chosen to be the lightest neutrino mass. δ , which appears multiplied by s_{13} , is beyond present experimental sensitivity. The sign of Δm_{31}^2 is not presently known, and could be negative (known as inverted hierarchy), however, in this case $|(m_\nu)_{ee}| > 10^{-2}$ eV and cannot be

accommodated within our model; we will therefore consider only the normal hierarchy case $\Delta m_{31}^2 > 0$. Finally, recent data on electron neutrino appearance at T2K [55] and Double Chooz [56] experiments point out to a mixing angle θ_{13} different from zero.

A possible way of identifying the allowed region in parameter space would be to first generate random values for masses, angles and phases within the 1σ regions experimentally allowed in Eqs. (38) and (39), and obtain scatter plots for m_ν . Then, using Eq. (33) we can solve for g_{ab} , up to an overall factor $\propto \mu_\kappa v_\chi^2 I_\nu / v_\phi^4$, and then find the values of $\mu_\kappa, v_\chi, m_\kappa, m_\chi$ which respect the constraints discussed in the previous sections. The potential problem we face is due to the specific form of the neutrino mass matrix, which contains $m_a g_{ab}^* m_b$ (see Eq. (33)), and is therefore suppressed for the first generations due to the light charged-lepton mass factors. To compensate this may require g_{ab} to be too large to meet the bounds required by $0\nu\beta\beta$ decay (Section III), LFV processes (Section IV) and perturbative unitarity (Appendix B). An alternative way to proceed is noticing that in practice (see (35) and (37)) we are asking if $|(m_\nu)_{ee,e\mu}| \sim 0$ is consistent with neutrino oscillation data (a question also of general interest not only within the model under consideration). These additional constraints will hold only within a limited region of the allowed neutrino masses and mixing parameters, which then implies that the type of models under consideration gives rather clear predictions about some of these parameters.

In order to see how this comes about it is useful to go through a straightforward parameter counting exercise: m_ν is a 3×3 complex and symmetric matrix specified by 12 real numbers: 3 of these are unphysical and can be absorbed in re-phasing the neutrino fields, and 5 of the remaining 9 are measured (2 mass differences and 3 mixing angles, where we include θ_{13}). If we now impose $(m_\nu)_{ee,e\mu} = 0$, corresponding to 4 additional (real) constraints, only a set of points (or narrow regions, allowing for experimental accuracy) will be consistent. In fact, there may be no allowed values at all! We have checked, however, that for each allowed choice of the experimentally measured parameters there is a unique solution for $\alpha_1, \alpha_2, \delta$ and m_1 satisfying all these restrictions. For example using the central values of the global fit given after Eq. (39) we find:

$$\alpha_1 = 0.65 \quad , \quad \alpha_2 = -2.32 \quad , \quad \delta = -0.78 \quad , \quad m_1 = 0.0036 \text{ eV} \quad , \quad (40)$$

with

$$m_\nu \approx 10^{-2} \begin{pmatrix} 0 & 0 & 0.59 + 0.58i \\ 0 & 2.47 - 0.2i & 2.64 + 0.2i \\ 0.59 + 0.58i & 2.64 + 0.2i & 2.12 - 0.21i \end{pmatrix} \text{ eV} . \quad (41)$$

This exercise can be repeated for different values of $\sin^2 \theta_{13}$, and the amazing result is that for the central values of $\Delta m_{21,31}^2$ and $s_{12,23}^2$ there are solutions only for $0.012 < \sin^2 \theta_{13} < 0.024$, a range of values that roughly coincides with the result obtained by the global fits to present data and by recent T2K and Double Chooz experiments. To illustrate this result we present in Fig. 4 the $\sin^2 \theta_{13} - \delta$ region allowed when $|(m_\nu)_{ee,e\mu}| = 0$ is imposed. The green, darker region is obtained when measured mixings and mass differences (except $\sin \theta_{13}$) are varied within 1σ , while the yellow, lighter one is obtained by varying them within 3σ . For comparison we also present the recent Double Chooz result [56] ($\sin^2(2\theta_{13}) = 0.085 \pm 0.029 \pm 0.042$, adding statistical and systematic errors quadratically we obtain $\sin^2 \theta_{13} = 0.022 \pm 0.013$) as a vertical band, while the cross stands for the reference point in Fig. 2.

Of course, $(m_\nu)_{ee}$ and $(m_\nu)_{e\mu}$ cannot be identically zero but small, $\lesssim 10^{-4}$ eV. In fact, g_{ee} must be different from zero and rather large in order to $0\nu\beta\beta$ decay be observable (in this type of models $(m_\nu)_{ee}$ is small due to the huge suppression factor m_e^2 entering in its expression, not because g_{ee} is small itself). When $(m_\nu)_{ee}$ and $(m_\nu)_{e\mu}$ are allowed to vary within the model, with the other parameters staying within their 1σ range, $\sin^2 \theta_{13}$ is no longer bounded from above although the lower bound remains:

$$\sin^2 \theta_{13} \gtrsim 0.008 . \quad (42)$$

In order to illustrate this behaviour we plot in Fig. 5 $|(m_\nu)_{e\mu}|$ as a function of $\sin^2 \theta_{13}$, with all the neutrino masses and other mixing parameters varying arbitrarily within their 1σ limits. The red, darker region corresponds to $|(m_\nu)_{ee}|$ less than $|(m_\nu)_{e\mu}|$. For comparison, we also plot the recent Double Chooz limit given above which is fully compatible with the T2K 90% C.L. interval $0.007 - 0.07$ [55], and in agreement with current global fits (for instance, the one used in this paper [54] allows for $0.008 < \sin^2 \theta_{13} < 0.020$ at 1σ). Analogously, in Fig. 6 we draw $|(m_\nu)_{ee}|$ as a function of the lightest neutrino mass m_1 . The red, darker region stands now for $|(m_\nu)_{e\mu}| < |(m_\nu)_{ee}|$. The previous figures are obtained from the neutrino mass restrictions only. But in our approach the model parameters are further constrained by the bounds from $0\nu\beta\beta$ decay and LFV processes, which, as already emphasized, require

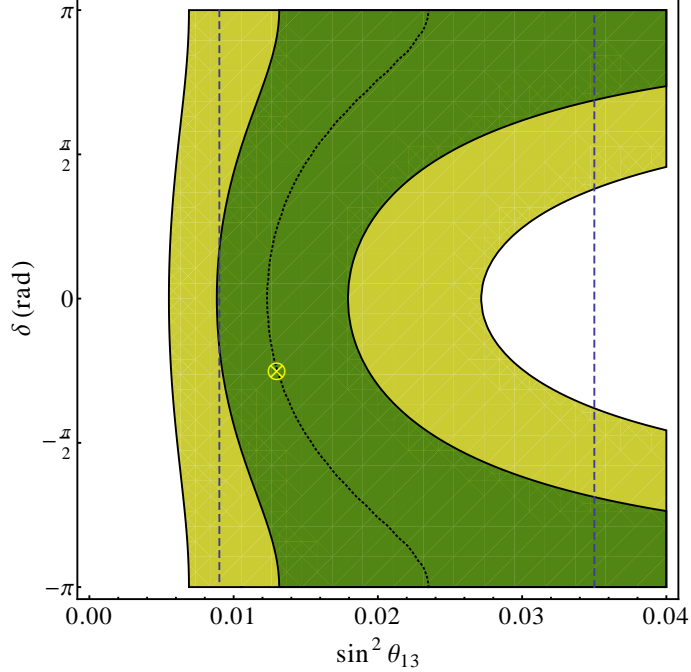


Figure 4: Allowed $\sin^2 \theta_{13} - \delta$ region for $|(m_\nu)_{ee,e\mu}| = 0$. The green, darker region is obtained when measured mixings and mass differences (except $\sin \theta_{13}$) are varied within 1σ ; while the yellow, lighter one is obtained by varying them within 3σ . The middle dotted curve corresponds to the central values of the neutrino masses and mixings in the global fit performed in Ref. [54]. For comparison, we also draw the recent Double Chooz [56] 1σ limits, where statistical and systematic errors are added in quadrature (vertical dashed lines). The cross stands for the reference point in Fig. 2.

$|(m_\nu)_{ee,e\mu}| \lesssim 10^{-4}$ (see Eqs. (35) and (37), respectively). Then, $\sin^2 \theta_{13} \gtrsim 0.008$ and $0.002 \text{ eV} \lesssim m_1 \lesssim 0.007 \text{ eV}$, as seen from Figs. 5 and 6, respectively. It then follows that a sufficiently precise measurement of $\sin \theta_{13}$ can exclude the model being discussed, as stressed before.

To conclude this section we derive the lower bounds, announced in Section III, on the scalar masses implied by the experimental limit on the $\tau^- \rightarrow e^+ \mu^- \mu^-$ branching ratio ($< 1.7 \times 10^{-8}$). In our model $|g_{\tau e} g_{\mu\mu}^*|$ must be large in order to reproduce the observed pattern of neutrino masses. More precisely,

$$|g_{e\tau} g_{\mu\mu}| = \frac{(2(2\pi)^4 v_\phi^4)^2 |(m_\nu)_{e\tau}| |(m_\nu)_{\mu\mu}|}{m_e m_\tau m_\mu^2 \mu_\kappa^2 v_\chi^4 I_\nu^2} \stackrel{\text{Pert}}{>} 0.065 \left(\frac{\text{TeV}}{I_\nu \min(m_{\kappa_{1,2}})} \right)^2, \quad (43)$$

where the second inequality follows from Eq. (27) and the substitution of the other variables

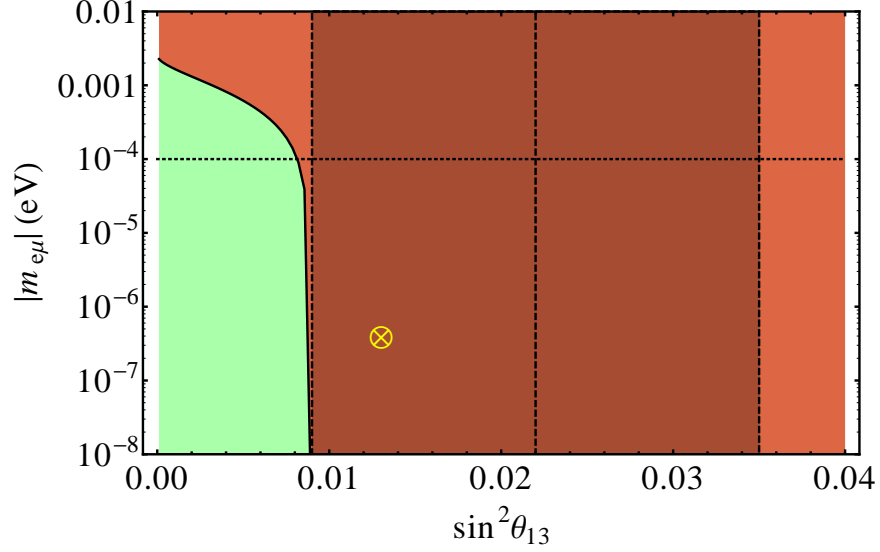


Figure 5: $|(m_\nu)_{e\mu}|$ as a function of $\sin^2\theta_{13}$. The green, lighter area which extends to all the panel is obtained varying the other measured masses and mixings within 1σ . The red, darker region satisfies the extra constraint $|(m_\nu)_{ee}| < |(m_\nu)_{e\mu}|$. The cross corresponds to the reference point in Fig. 2, and can be reached with either condition $|(m_\nu)_{ee}| \lesseqgtr |(m_\nu)_{e\mu}|$; whereas the darkest vertical 1σ band stands for the recent Double Chooz result, summing errors in quadrature. We also draw the line $|(m_\nu)_{e\mu}| = 10^{-4}$, which is the upper-limit estimate in this model.

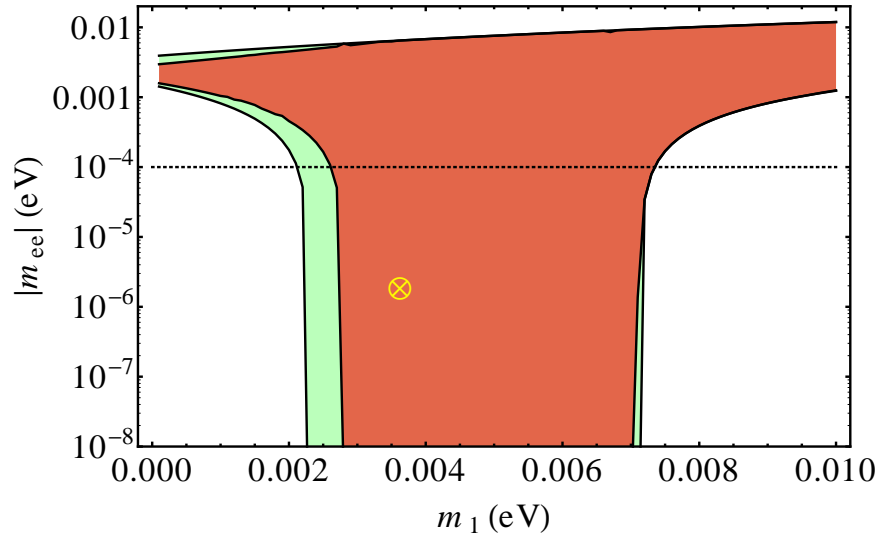


Figure 6: $|(m_\nu)_{ee}|$ as a function of m_1 . Similarly to Fig. 5, but with the red, darker region instead satisfying the extra constraint $|(m_\nu)_{e\mu}| < |(m_\nu)_{ee}|$. We also draw the line $|(m_\nu)_{ee}| = 10^{-4}$, which is the upper-limit estimate in this model.

by their approximate values (see, for instance, Eq. (41) for the $|(m_\nu)_{e\tau,\mu\mu}|$ estimates), in particular $v_\chi < 2$ GeV. Then, using Eq. (29) for $\tau^- \rightarrow e^+\mu^-\mu^-$ and the experimental limit on its branching ratio one obtains $|g_{e\tau}g_{\mu\mu}| < 0.007(m_\kappa/\text{TeV})^2$, which combined with Eq. (43) yields $m_\kappa > 1.2$ TeV (see Fig. 2, left)¹². We will present a detailed study of LFV processes in this type of models elsewhere.

VI. COLLIDER SIGNALS

Direct evidence for this type of models would be the discovery of the new scalars at a large collider. Doubly-charged scalars have fixed couplings to photons and are then produced at colliders with known cross sections. In addition their decay into leptons offers a very clean signal, which is particularly important at hadronic machines. Therefore, if doubly-charged scalars are light enough, they are very well suited for detection at colliders.

In general, this type of scalars is assumed to be part of a weak triplet, and usually also acts as see-saw messenger of type II generating tree-level Majorana masses for the light neutrinos [46–48, 57] (see also [58]). Such triplets are then well-motivated on theoretical grounds, especially when considering LR symmetric models, and studies for searching the corresponding doubly-charged scalars at future colliders have been performed in the past [59–63] (see also [64, 65] for recent studies; model independent studies have also been carried out in the literature [66, 67]). The general conclusion is that the LHC discovery limit reaches masses over 600 GeV (for a center of mass energy of 14 TeV and an integrated luminosity of 30 fb^{-1}) [64, 68]. However, the actual limits may be much better given the outstanding LHC performance, which almost matches the most favourable expectations for a CM energy of 7 TeV [69]. (See for a review [70].)

Recently, first results from CMS have been presented at a CM energy of 7 TeV with an integrated luminosity of 0.89 fb^{-1} [71]. The analysis assumed a scalar triplet coupled to leptons, with 100% branching ratio to each leptonic channel. Nothing is seen, leading to a lower bound on the doubly-charged scalar mass of about 250 GeV if the main decay channel contain τ leptons, and to about 300 GeV if they contain only electrons or muons. Weaker limits were obtained previously by LEP and the Tevatron. The absence at LEP of a pair-

¹² Note that we have used $I_\nu \sim 2$ because m_χ is somewhat larger than m_κ (see Appendix C).

production signal ($e^+e^- \rightarrow \gamma^*, Z^* \rightarrow \kappa\bar{\kappa}$) gives the constraint $m_\kappa > 100$ GeV [72–74]¹³. Limits on this type of scalars have been also derived using Tevatron data [76–78], leading to a limit $m_\kappa > 100 - 150$ GeV (depending on the details of the model).

In our model the triplet does not directly couple to fermions, while the doubly-charged singlet does not couple to W pairs; however, triplet and singlet mix. Of the resulting mass eigenstates one, κ_1 , is mainly a singlet and decays dominantly to lepton pairs, while the other, κ_2 , is mainly a triplet and has suppressed couplings to charged leptons. Both of them can be produced at LHC via the Drell-Yan mechanism ($q\bar{q} \rightarrow \gamma^*, Z^* \rightarrow \kappa^{++}\kappa^{--}$) with full strength. Since this is the main production process considered by CMS, the former limits apply directly to κ_1 for a non-negligible mixing: $300 \text{ GeV} < m_{\kappa_1}$. Limits on m_{κ_2} will be more difficult to obtain since the process $q\bar{q} \rightarrow \gamma^*, Z^* \rightarrow \kappa_2\bar{\kappa}_2 \rightarrow W^+W^+W^-W^-$ is much more complicated to deal with, due to its large backgrounds and the in general difficult reconstruction of several leptonic W decays.

Notice that there are other production processes that are more model dependent. In particular, the same interaction that induces $0\nu\beta\beta$ decay and the decay of κ into gauge bosons can mediate single-scalar production through WW fusion. The amplitude is proportional to the triplet VEV, v_χ , which is small, and to the singlet-triplet mixing, $\sin\theta_D$, further suppressing this process. Nonetheless this could prove to be the dominant production channel at LHC [60] if $v_\chi > 1$ GeV and $m_{\kappa_{1,2}} > 500$ GeV. This is especially relevant for our model since both LHC and low-energy constraints require a relatively large v_χ as well as large scalar masses (see Fig. 2), all of which is in marked contrast to the constraints on triplet models with tree-level type II see-saw neutrino masses. A thorough study of the various possibilities is somewhat involved [79] and lies outside the scope of this paper; we will revisit these aspects of our model in a future publication.

VII. CONCLUSIONS

In this paper we have presented a simple model with a large $0\nu\beta\beta$ decay rate into RH electrons through the exchange of the SM W boson and new heavy scalars κ, χ . In this

¹³ Single production via $e^+e^- \rightarrow \kappa ee$, as well the u -channel contribution of κ to Bhabha scattering have also been studied at LEP [74, 75], but the corresponding bounds depend on the unknown values of the Yukawa couplings.

model the light neutrino masses, $0\nu\beta\beta$ decay and LFV processes have a common origin, which provides a simple description of these processes and also leads to a rather constrained parameter space. A $0\nu\beta\beta$ decay final state with RH electrons also occurs in left-right (LR) models (see [80] for a detailed discussion), but generated by the exchange of new heavy neutrinos N and gauge bosons W_R . In these models this process is a priori decoupled from the light neutrino mass generation, and hence the rate for $0\nu\beta\beta$ decay can be large and at the same time the effective electron mass $(m_\nu)_{ee}$ small. Despite these differences both types of models have similar low-energy (below the electroweak scale) limits or, equivalently, they represent very different UV completions of two similar effective Lagrangians at scales below m_W . A general discussion of the different alternatives using an effective Lagrangian approach is presented in a companion paper [16].

The specific model we have discussed is one of a wide class of theories with similar phenomenology. For example, we choose to break LN explicitly by introducing one neutral scalar singlet (σ), but, as discussed in Section II we could promote σ to a complex singlet and insure the Lagrangian is LN invariant, and this symmetry spontaneously broken; while the neutrino phenomenology remains similar, it is simpler to discuss in our case. In general, this class of models require several new scalar multiplets to allow for non-vanishing scalar couplings to RH electrons, together with a chain of scalar couplings connecting them to the standard gauge boson triplet, and if desired, to the SM Higgs doublet in order to relate the new LN acting on the RH leptons to the ordinary LN associated with LH leptons. In such cases $0\nu\beta\beta$ decay into RH electrons and the light neutrino Majorana masses are again related although at different loop order, as in our model.

This model, which we considered in some detail, is based on an extended scalar sector containing three new multiplets: two isosinglets and one isotriplet, the physical spectrum contains two light scalars (with masses $\sim v_{\phi,\sigma}$) and 5 heavy scalars (with masses $O(\text{TeV})$): 2 doubly-charged, 1 singly-charged and 2 neutral. After writing the corresponding scalar potential and showing that there is a region of parameter space allowing for a local minimum along the desired direction, we have elaborated on their low-energy phenomenological implications. In deriving our quantitative predictions we required for the model to remain perturbative up to several tens of TeV.

As repeatedly stressed, the new scalars mediate $0\nu\beta\beta$ decay into RH electrons, LFV processes and, at two loops, generate Majorana neutrino masses. By requiring $0\nu\beta\beta$ decay

to be large enough to be observable at the next round of experiments, we have derived lower bounds on the coupling to RH electrons g_{ee} and upper bounds on the masses of the exchanged scalars. On the other hand, the stringent experimental limits on LFV transitions (particularly $\mu^- \rightarrow e^+ e^- e^-$ and $\tau^- \rightarrow e^+ \mu^- \mu^-$) translate into upper bounds on the couplings g_{ab} and lower bounds on the masses of the new particles involved, and these create some tension with the assumed $0\nu\beta\beta$ decay rate. As a result, the model predicts that most LFV processes can be within the reach of the next generation of experiments, too.

These same couplings and masses also enter the (two-loop) expression for the Majorana neutrino masses that have the very characteristic form, $(m_\nu)_{ab} \propto m_a g_{ab}^* m_b$, proportional to the scalar couplings to two RH leptons g_{ab} and to the corresponding charged lepton masses $m_{a,b}$. Accommodating the observed neutrino mass spectrum and mixing parameters together with the other constraints is possible, but only for very restricted values of the lightest neutrino mass (not testable in neutrino oscillation experiments), and when the mixing angle θ_{13} is constrained to lie within the preferred 1σ range from the global fit in Ref. [54], $0.008 < \sin^2 \theta_{13} < 0.020$. This last prediction also goes far beyond our model, and holds whenever the (symmetric) neutrino mass matrix contains three very small entries, for example, $m_{ee}, m_{e\mu}(= m_{\mu e}) \sim 0$, as in our case ¹⁴. Some of these constraints can be alleviated by further extending the scalar sector, although at the price of requiring precise cancellations (that could be naturally enforced using further symmetries).

The model considered presents a simple consistent extension of the SM exhibiting a large $0\nu\beta\beta$ decay, but where the contributions to this decay generated by the neutrino Majorana masses are negligible. The neutrino masses themselves are predictable, in contrast with other proposals (see, for example [84]), and consistent with existing data. Note, however, that although our phenomenological approach and the constraints on the model mainly follow from requiring an observable $0\nu\beta\beta$ in the next round of experiments, the non-observation of this decay and even a vanishing decay rate would be compatible with our analysis. That would be the case for $g_{ee} \rightarrow 0$, value which would also ease the LFV restrictions without altering the neutrino mass predictions. As they are obtained assuming that $(m_\nu)_{ee}$, which is proportional to g_{ee} , too, is to a large extent negligible.

¹⁴ A general discussion of the implications of texture zeroes in neutrino mass matrices can be found in [81, 82], and most recently in [83].

Finally, we have also reviewed the collider limits on doubly-charged scalars. The excellent LHC performance should soon allow for the actual confrontation with the expected masses and couplings for the new scalars in the type of models studied here. We must, anyhow, be aware that once LHC settles the fate of the SM Higgs boson¹⁵, the mass and couplings of the scalar doublet will be further constrained, implying further restrictions in the scalar potential which must be checked that can be satisfied. At any rate, the model studied here is one of a wider class sharing the main assumption in our analysis, that $0\nu\beta\beta$ decay is large and decoupled from any mechanism providing tree-level neutrino masses, although the latter are generated through higher-order radiative corrections.

Appendix A: Bound on the scalar triplet VEV

As it is well known, the VEV of a triplet with hypercharge 1 gives a tree-level contribution to the ρ parameter, spoiling the successful SM (tree-level) prediction $\rho_0 = 1$. In general,

$$\rho_0 = \frac{\sum_i v_i^2 [T_i(T_i + 1) - Y_i^2]}{\sum_i 2v_i^2 Y_i^2}, \quad (\text{A1})$$

where the sum runs over the scalars of isospin T_i and hypercharge Y_i with VEV v_i . For the case under consideration, and assuming that the VEV of the triplet is much smaller than the one of the doublet,

$$\rho_0 = \frac{v_\phi^2 + 2v_\chi^2}{v_\phi^2 + 4v_\chi^2} \approx 1 - \frac{2v_\chi^2}{v_\phi^2}. \quad (\text{A2})$$

Then, the VEV of the scalar triplet contributes negatively to ρ_0 , while the best ρ value obtained from a global fit to electroweak precision data is [1] $\rho = 1.0008_{-0.0010}^{+0.0017}$ at 1σ , and $\rho = 1.0004_{-0.0011}^{+0.0023}$ at 2σ . Thus, $v_\chi^2/v_\phi^2 < 0.00035$ at 2σ , implying $v_\chi < 3\text{ GeV}$ for $v_\phi \approx 174\text{ GeV}$. Which is comparable to the bound derived from the global fit including explicitly the scalar triplet effects, $v_\chi < 2\text{ GeV}$ at the 90% C.L. [88].

However, a more complete analysis should also include the radiative corrections to the ρ parameter induced, for example, by the exchange of the scalar triplet, which can be positive [89]. For instance, in the triplet Majoron model [90] $\Delta\rho = \frac{(1 - \ln 2)}{2\pi^2\sqrt{2}} G_F m_\chi^2$, with

¹⁵ In the very near future the LHC will be able to exclude a heavy Higgs with a relatively large significance [85, 86] but electroweak precision data do prefer a light Higgs (see, for instance, Ref. [87] and references there in), which shall require further for confirmation (or exclusion).

m_χ the mass of the doubly-charged scalar, cancelling partially the tree-level contribution. Since these contributions depend on the mass splitting of the triplet components, which in our model is not fixed, we will assume a conservative upper bound

$$v_\chi < 5 \text{ GeV} . \tag{A3}$$

Appendix B: Constraints from naturality and perturbative unitarity

The relevant parameter for $0\nu\beta\beta$ decay and neutrino masses is the product of couplings and VEVs $\mu_\kappa v_\chi^2 g_{ee}$. It cannot be too large without leaving the perturbative regime and there are different arguments that can be used to set upper limits on its size (perturbative unitarity, naturality, etc.).

Let us discuss the constraints from perturbative unitarity. Consider first the Yukawa couplings of doubly-charged scalars. Tree-level unitarity at high energy, $s \gg m_{\kappa_{1,2}}$, in $ee \rightarrow ee$ collisions mediated by $\kappa_{1,2}$ requires $|g_{ee}| < \sqrt{4\pi}$. Similar bounds can be obtained from other channels. In order to be definite, we will demand

$$|g_{\alpha\beta}|^{\text{Pert}} < \sqrt{4\pi} . \tag{B1}$$

Tree-level unitarity at high energy does not give useful information on dimensional parameters like μ_κ because amplitudes involving these couplings decrease with energy. However, it does not seem natural to have μ_κ much larger than other dimensionful parameters in the model, like m_κ or m_χ . In fact, one-loop diagrams involving the μ_κ coupling give contributions to m_κ or m_χ which are of order $\delta m_{\kappa,\chi} \sim \mu_\kappa^2 / (4\pi)^2$. Therefore, it seems appropriate to require

$$\mu_\kappa^{\text{Pert}} < 4\pi \min(m_{\kappa_{1,2}}) . \tag{B2}$$

Limits (B1) and (B2) also guarantee that the κ_1 decay width (to leptons and to κ_2 , if this is light enough) is not too large as compared to its mass.

One must be aware, however, that all these limits are estimates which depend on the naturality approach. Thus, although at the price of fine tuning, one might decide to fix the model parameters outside the range defined by these limits. Moreover, there can be model extensions where those values are natural. At any rate, we use Eqs. (B1) and (B2) in the text to illustrate that the allowed regions in parameter space are at a large extent bounded if the perturbative theory must stay natural.

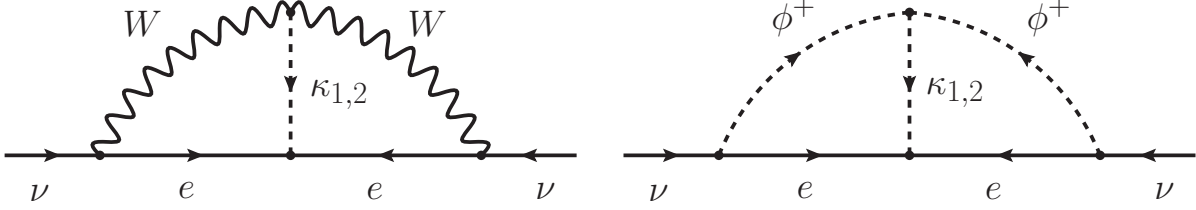


Figure 7: Two-loop diagrams contributing to neutrino masses in the generalized R_ξ gauge.

Appendix C: Loop integrals for evaluating neutrino masses

The evaluation of the complete two-loop contribution to neutrino masses, including m_W effects in a general R_ξ gauge, is a complicated task. Fortunately, we found a gauge in which the calculation simplifies enormously. Indeed, one can choose a gauge in which triplet and doublet charged scalars do not mix at all (the gauge-fixing Lagrangian is of the form $\mathcal{L}_{\text{gf}} = a|\partial \cdot W^+ + b\chi^+ + c\phi^+|^2$ with the constants a, b, c chosen to cancel the $\phi^+\chi^-$ and the $W^+\chi^-, W^+\phi^-$ mixing terms). In this gauge the charged Goldstone boson becomes degenerate with the physical charged scalar; and ω^\pm does not couple to fermions, whereas G^\pm does not have derivative couplings to the doubly-charged scalars and gauge bosons. Therefore, the only diagrams contributing to neutrino masses are those depicted in Fig. 7. (The corresponding Feynman rules are obtained redefining the fields in Section II A adequately; in particular, in this gauge $\omega^\pm = \chi^\pm$ and $G^\pm = \phi^\pm$.) Following the notation in Eq. (33) we will have now $I_\nu = I_W + I_\phi$, where I_W and I_ϕ are the two contributions from the diagrams in Fig. 7. They read

$$I_W = -2(4\pi)^4 m_W^4 \cos^4 \theta_S \int \frac{1}{k^2(k^2 - m_W^2)q^2(q^2 - m_W^2)((k - q)^2 - m_{\kappa_1}^2)((k - q)^2 - m_{\kappa_2}^2)} \times \\ \times \left(4 - \left(1 - \frac{m_\omega^2}{m_W^2} \right) \left(\frac{k^2}{k^2 - m_\omega^2} + \frac{q^2}{q^2 - m_\omega^2} \right) + \left(1 - \frac{m_\omega^2}{m_W^2} \right)^2 \frac{(k \cdot q)^2}{(k^2 - m_\omega^2)(q^2 - m_\omega^2)} \right), \quad (\text{C1})$$

$$I_\phi = (4\pi)^4 \frac{m_A^2}{\cos^2 \theta_I} \int \frac{k \cdot q}{k^2(k^2 - m_\omega^2)q^2(q^2 - m_\omega^2)((k - q)^2 - m_{\kappa_1}^2)((k - q)^2 - m_{\kappa_2}^2)},$$

where in I_ϕ we used the equality $v_\chi m_A^2 = -\lambda_6 v_\sigma v_\phi^2 \cos^2 \theta_I$ (see Section II) to rewrite λ_6 in terms of m_A . Note also that both doubly-charged scalar masses must enter symmetrically in the integrals to obtain a non-vanishing contribution.

We have checked that in the decoupling limit ($m_W \ll m_{\kappa_1, \kappa_2, \omega, A}$ and $v_\chi \ll v_\phi$, implying $m_{\kappa_2} = m_\omega = m_\chi$ and $\cos \theta_S = \cos \theta_I = 1$) we recover the results obtained in the mass

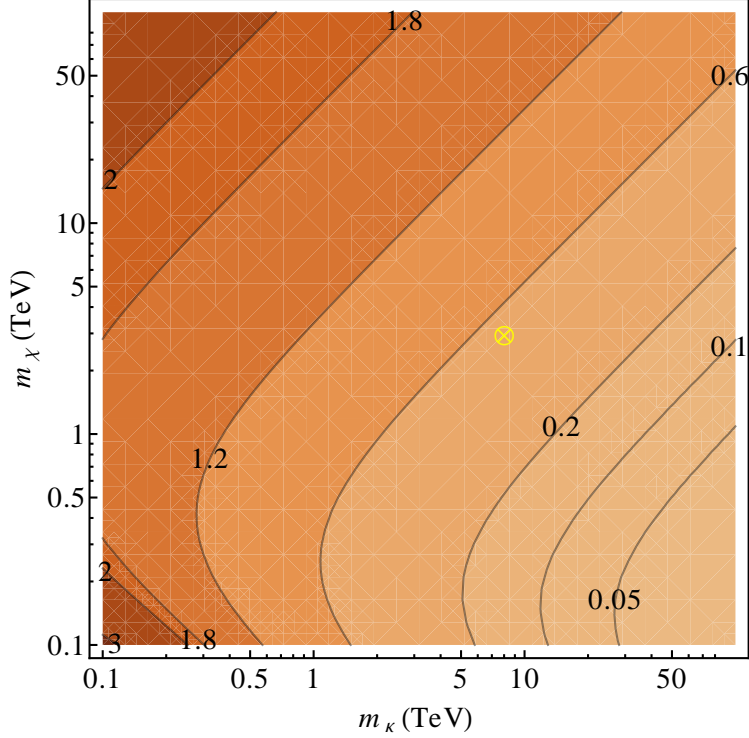


Figure 8: Contour plot for the loop integral I_ν as a function of the masses $m_{\kappa_1} \approx m_\kappa$ and $m_{\kappa_2} \approx m_\chi$ for $m_W = 80$ GeV and $m_\omega = m_A = m_{\kappa_2}$. The cross denotes the reference point in the text.

insertion approximation discussed in Section V. In general I_ν is a complicated function of $m_W, m_{\kappa_1, \kappa_2, \omega, A}$ and the ratio v_χ/v_ϕ , which defines $\cos\theta_S$ and $\cos\theta_I$. However, since $v_\chi \ll v_\phi$, we can safely neglect the corresponding corrections (in the limit of large m_χ the triplet VEV v_χ is small, and so is then the mixing of the triplet components with doublets and singlets; analogously, the contribution of doublet and singlet VEVs to the masses of the triplet components can be ignored). In this case I_ν becomes a function only of $m_{\kappa_1}^2/m_W^2$ and $m_{\kappa_2}^2/m_W^2$ that we compute numerically. In Fig. (8) we plot the contours of constant I_ν as a function of the masses $m_{\kappa_1} \approx m_\kappa$ and $m_{\kappa_2} \approx m_\chi$, where we have fixed $m_W = 80$ GeV. From the Figure we see that I_ν is order one for a large region of the parameter space. Only when $m_{\kappa_1} \gg m_{\kappa_2}$ there is some suppression. The cross corresponds to the value of the reference point in Section III.

Acknowledgments

This work has been supported in part by the Ministry of Science and Innovation (MICINN) Spain, under the grant numbers FPA2006-05294, FPA2008-03373, FPA2010-17915 and FPA2011-23897, by the Junta de Andalucía grants FQM 101, FQM 03048 and FQM 6552, by the “Generalitat Valenciana” grant PROMETEO/2009/128 and by the U.S. Department of Energy grant No. DE-FG03-94ER40837. A.A. is supported by the MICINN under the FPU program.

-
- [1] **Particle Data Group** Collaboration, K. Nakamura *et al.*, *Review of particle physics*, *J.Phys.G* **G37** (2010) 075021 [[InSPIRE](#)].
 - [2] M. Gonzalez-Garcia and M. Maltoni, *Phenomenology with Massive Neutrinos*, *Phys.Rept.* **460** (2008) 1–129, [[arXiv:0704.1800](#)] [[InSPIRE](#)].
 - [3] R. Mohapatra, S. Antusch, K. Babu, G. Barenboim, M.-C. Chen, *et al.*, *Theory of neutrinos: A White paper*, *Rept.Prog.Phys.* **70** (2007) 1757–1867, [[arXiv:hep-ph/0510213](#)] [[InSPIRE](#)].
 - [4] G. Altarelli and F. Feruglio, *Neutrino masses and mixings: A theoretical perspective*, *Phys.Rept.* **320** (1999) 295–318 [[InSPIRE](#)].
 - [5] B. Pontecorvo, *Neutrino Experiments and the Problem of Conservation of Leptonic Charge*, *Sov.Phys.JETP* **26** (1968) 984–988 [[InSPIRE](#)].
 - [6] Z. Maki, M. Nakagawa, and S. Sakata, *Remarks on the unified model of elementary particles*, *Prog.Theor.Phys.* **28** (1962) 870–880 [[InSPIRE](#)].
 - [7] S. Weinberg, *Baryon and Lepton Nonconserving Processes*, *Phys.Rev.Lett.* **43** (1979) 1566–1570 [[InSPIRE](#)].
 - [8] W. Furry, *On transition probabilities in double beta-disintegration*, *Phys.Rev.* **56** (1939) 1184–1193 [[InSPIRE](#)].
 - [9] M. Fukugita and T. Yanagida, *Baryogenesis Without Grand Unification*, *Phys.Lett.* **B174** (1986) 45 [[InSPIRE](#)].
 - [10] S. Davidson, E. Nardi, and Y. Nir, *Leptogenesis*, *Phys.Rept.* **466** (2008) 105–177, [[arXiv:0802.2962](#)] [[InSPIRE](#)].
 - [11] G. Branco, R. Felipe, and F. Joaquim, *Leptonic CP violation*, [[arXiv:1111.5332](#)] [[InSPIRE](#)].

- [12] J. Vergados, *The Neutrinoless double beta decay from a modern perspective*, *Phys.Rept.* **361** (2002) 1–56, [[arXiv:hep-ph/0209347](#)] [[InSPIRE](#)].
- [13] J. Schechter and J. Valle, *Neutrinoless Double beta Decay in $SU(2) \times U(1)$ Theories*, *Phys.Rev.* **D25** (1982) 2951 [[InSPIRE](#)].
- [14] A. Barabash, *Double beta decay experiments*, *Phys.Part.Nucl.* **42** (2011) 613–627, [[arXiv:1107.5663](#)] [[InSPIRE](#)].
- [15] I. Avignone, Frank T., S. R. Elliott, and J. Engel, *Double Beta Decay, Majorana Neutrinos, and Neutrino Mass*, *Rev.Mod.Phys.* **80** (2008) 481–516, [[arXiv:0708.1033](#)] [[InSPIRE](#)].
- [16] F. del Aguila, A. Aparici, S. Bhattacharya, A. Santamaria, and J. Wudka, *Effective Lagrangian approach to neutrinoless double beta decay and neutrino masses*. CAFPE-166/11, UG-FT-296/11, FTUV-11-1212, IFIC/11-66, 2011.
- [17] K. Babu and C. N. Leung, *Classification of effective neutrino mass operators*, *Nucl.Phys.* **B619** (2001) 667–689, [[arXiv:hep-ph/0106054](#)] [[InSPIRE](#)].
- [18] K.-w. Choi, K. S. Jeong, and W. Y. Song, *Operator analysis of neutrinoless double beta decay*, *Phys.Rev.* **D66** (2002) 093007, [[arXiv:hep-ph/0207180](#)] [[InSPIRE](#)].
- [19] J. Engel and P. Vogel, *Effective operators for double beta decay*, *Phys.Rev.* **C69** (2004) 034304, [[arXiv:nucl-th/0311072](#)] [[InSPIRE](#)].
- [20] A. de Gouvea and J. Jenkins, *A Survey of Lepton Number Violation Via Effective Operators*, *Phys. Rev.* **D77** (2008) 013008, [[arXiv:0708.1344](#)] [[InSPIRE](#)].
- [21] C.-S. Chen, C. Geng, and J. Ng, *Unconventional Neutrino Mass Generation, Neutrinoless Double Beta Decays, and Collider Phenomenology*, *Phys.Rev.* **D75** (2007) 053004, [[arXiv:hep-ph/0610118](#)] [[InSPIRE](#)].
- [22] C.-S. Chen, C.-Q. Geng, J. N. Ng, and J. M. Wu, *Testing radiative neutrino mass generation at the LHC*, *JHEP* **0708** (2007) 022, [[arXiv:0706.1964](#)] [[InSPIRE](#)].
- [23] R. Mohapatra and P. Pal, *Massive neutrinos in physics and astrophysics*, *World Sci.Lect.Notes Phys.* **60** (1998) 1–397 [[InSPIRE](#)].
- [24] A. Atre, T. Han, S. Pascoli, and B. Zhang, *The Search for Heavy Majorana Neutrinos*, *JHEP* **0905** (2009) 030, [[arXiv:0901.3589](#)] [[InSPIRE](#)].
- [25] A. Ibarra, E. Molinaro, and S. Petcov, *TeV Scale See-Saw Mechanisms of Neutrino Mass Generation, the Majorana Nature of the Heavy Singlet Neutrinos and $(\beta\beta)_{0\nu}$ -Decay*, *JHEP* **1009** (2010) 108, [[arXiv:1007.2378](#)] [[InSPIRE](#)].

- [26] M. Mitra, G. Senjanovic, and F. Vissani, *Neutrinoless Double Beta Decay and Heavy Sterile Neutrinos*, *Nucl.Phys.* **B856** (2012) 26–73, [[arXiv:1108.0004](#)] [[InSPIRE](#)].
- [27] M. Blennow, E. Fernandez-Martinez, J. Lopez-Pavon, and J. Menendez, *Neutrinoless double beta decay in seesaw models*, *JHEP* **1007** (2010) 096, [[arXiv:1005.3240](#)] [[InSPIRE](#)].
- [28] J. C. Pati and A. Salam, *Lepton Number as the Fourth Color*, *Phys.Rev.* **D10** (1974) 275–289 [[InSPIRE](#)].
- [29] R. Mohapatra and J. C. Pati, *A Natural Left-Right Symmetry*, *Phys.Rev.* **D11** (1975) 2558 [[InSPIRE](#)].
- [30] G. Senjanovic and R. N. Mohapatra, *Exact Left-Right Symmetry and Spontaneous Violation of Parity*, *Phys.Rev.* **D12** (1975) 1502 [[InSPIRE](#)].
- [31] M. Duerr, M. Lindner, and A. Merle, *On the Quantitative Impact of the Schechter-Valle Theorem*, *JHEP* **1106** (2011) 091, [[arXiv:1105.0901](#)] [[InSPIRE](#)].
- [32] A. Zee, *Quantum numbers of Majorana neutrino masses*, *Nucl.Phys.* **B264** (1986) 99 [[InSPIRE](#)].
- [33] K. Babu, *Model of 'Calculable' Majorana Neutrino Masses*, *Phys.Lett.* **B203** (1988) 132 [[InSPIRE](#)].
- [34] Y. Zeldovich, I. Kobzarev, and L. Okun, *Cosmological Consequences of the Spontaneous Breakdown of Discrete Symmetry*, *Zh.Eksp.Teor.Fiz.* **67** (1974) 3–11 [[InSPIRE](#)].
- [35] A. Vilenkin, *Cosmic Strings and Domain Walls*, *Phys.Rept.* **121** (1985) 263 [[InSPIRE](#)].
- [36] R. E. Shrock and M. Suzuki, *Invisible decays of Higgs bosons*, *Phys.Lett.* **B110** (1982) 250 [[InSPIRE](#)].
- [37] S. Bertolini and A. Santamaria, *The stability of the VEV hierarchy and Higgs invisibility in Majoron models*, *Phys.Lett.* **B213** (1988) 487 [[InSPIRE](#)].
- [38] A. Aparici, K. Kim, A. Santamaria, and J. Wudka, *Right-handed neutrino magnetic moments*, *Phys.Rev.* **D80** (2009) 013010, [[arXiv:0904.3244](#)] [[InSPIRE](#)].
- [39] Y. Chikashige, R. N. Mohapatra, and R. Peccei, *Are There Real Goldstone Bosons Associated with Broken Lepton Number?*, *Phys.Lett.* **B98** (1981) 265 [[InSPIRE](#)].
- [40] K. Ghosh, B. Mukhopadhyaya, and U. Sarkar, *Signals of an invisibly decaying Higgs in a scalar dark matter scenario: a study for the Large Hadron Collider*, *Phys.Rev.* **D84** (2011) 015017, [[arXiv:1105.5837](#)] [[InSPIRE](#)].
- [41] K. Choi and A. Santamaria, *Majorons and Supernova Cooling*, *Phys.Rev.* **D42** (1990)

- 293–306 [[InSPIRE](#)].
- [42] Y. Chikashige, R. N. Mohapatra, and R. Peccei, *Spontaneously Broken Lepton Number and Cosmological Constraints on the Neutrino Mass Spectrum*, *Phys.Rev.Lett.* **45** (1980) 1926 [[InSPIRE](#)].
- [43] K. Choi and A. Santamaria, *17-KeV neutrino in a singlet - triplet majoron model*, *Phys.Lett.* **B267** (1991) 504–508 [[InSPIRE](#)].
- [44] P.-H. Gu, E. Ma, and U. Sarkar, *Pseudo-Majoron as Dark Matter*, *Phys.Lett.* **B690** (2010) 145–148, [[arXiv:1004.1919](#)] [[InSPIRE](#)].
- [45] L. Basso, *Phenomenology of the minimal B-L extension of the Standard Model at the LHC*, [[arXiv:1106.4462](#)] [[InSPIRE](#)].
- [46] W. Konetschny and W. Kummer, *Nonconservation of Total Lepton Number with Scalar Bosons*, *Phys.Lett.* **B70** (1977) 433 [[InSPIRE](#)].
- [47] T. Cheng and L.-F. Li, *Neutrino Masses, Mixings and Oscillations in SU(2) x U(1) Models of Electroweak Interactions*, *Phys.Rev.* **D22** (1980) 2860 [[InSPIRE](#)].
- [48] J. Schechter and J. Valle, *Neutrino Masses in SU(2) x U(1) Theories*, *Phys.Rev.* **D22** (1980) 2227 [[InSPIRE](#)].
- [49] H. Pas, M. Hirsch, H. Klapdor-Kleingrothaus, and S. Kovalenko, *A Superformula for neutrinoless double beta decay. 2. The Short range part*, *Phys.Lett.* **B498** (2001) 35–39, [[arXiv:hep-ph/0008182](#)] [[InSPIRE](#)].
- [50] M. Nebot, J. F. Oliver, D. Palao, and A. Santamaria, *Prospects for the Zee-Babu Model at the CERN LHC and low energy experiments*, *Phys.Rev.* **D77** (2008) 093013, [[arXiv:0711.0483](#)] [[InSPIRE](#)].
- [51] M. Raidal and A. Santamaria, *Muon electron conversion in nuclei versus $\mu \rightarrow e\gamma$: An Effective field theory point of view*, *Phys.Lett.* **B421** (1998) 250–258, [[arXiv:hep-ph/9710389](#)] [[InSPIRE](#)].
- [52] S. M. Bilenky, J. Hosek, and S. Petcov, *On Oscillations of Neutrinos with Dirac and Majorana Masses*, *Phys.Lett.* **B94** (1980) 495 [[InSPIRE](#)].
- [53] S. M. Bilenky and S. Petcov, *Massive Neutrinos and Neutrino Oscillations*, *Rev.Mod.Phys.* **59** (1987) 671 [[InSPIRE](#)].
- [54] T. Schwetz, M. Tortola, and J. Valle, *Where we are on θ_{13} : addendum to 'Global neutrino data and recent reactor fluxes: status of three-flavour oscillation parameters'*, *New J.Phys.* **13**

- (2011) 109401, [[arXiv:1108.1376](#)] [[INSPIRE](#)].
- [55] **T2K Collaboration** Collaboration, K. Abe *et al.*, *Indication of Electron Neutrino Appearance from an Accelerator-produced Off-axis Muon Neutrino Beam*, *Phys.Rev.Lett.* **107** (2011) 041801, [[arXiv:1106.2822](#)] [[INSPIRE](#)].
- [56] **Double Chooz** Collaboration, *First results from the Double Chooz experiment*. Presented at LowNu2011, 9-12 November, 2011, 2011.
<http://www.dchooz.org/DocDB/cgi-bin/public/ShowDocument?docid=3393>.
- [57] G. Gelmini and M. Roncadelli, *Left-Handed Neutrino Mass Scale and Spontaneously Broke n Lepton Number*, *Phys.Lett.* **B99** (1981) 411 [[INSPIRE](#)].
- [58] E. Ma and U. Sarkar, *Neutrino masses and leptogenesis with heavy Higgs triplets*, *Phys.Rev.Lett.* **80** (1998) 5716–5719, [[arXiv:hep-ph/9802445](#)] [[INSPIRE](#)].
- [59] J. Gunion, J. Grifols, A. Mendez, B. Kayser, and F. I. Olness, *Higgs Bosons in Left-Right Symmetric Models*, *Phys.Rev.* **D40** (1989) 1546 [[INSPIRE](#)].
- [60] K. Huitu, J. Maalampi, A. Pietila, and M. Raidal, *Doubly charged Higgs at LHC*, *Nucl.Phys.* **B487** (1997) 27–42, [[arXiv:hep-ph/9606311](#)] [[INSPIRE](#)].
- [61] J. F. Gunion, C. Loomis, and K. T. Pitts, *Searching for doubly charged Higgs bosons at future colliders*, in *In the Proceedings of 1996 DPF / DPB Summer Study on New Directions for High-Energy Physics (Snowmass 96)*, Snowmass, Colorado, 25 Jun - 12 Jul 1996, pp LTH096. Also in **Snowmass 1996, New directions for high-energy physics** 603-607. 1996. [[arXiv:hep-ph/9610237](#)]. [[INSPIRE](#)].
- [62] A. Akeroyd and M. Aoki, *Single and pair production of doubly charged Higgs bosons at hadron colliders*, *Phys.Rev.* **D72** (2005) 035011, [[arXiv:hep-ph/0506176](#)] [[INSPIRE](#)].
- [63] G. Azuelos, K. Benslama, and J. Ferland, *Prospects for the search for a doubly-charged Higgs in the left-right symmetric model with ATLAS*, *J.Phys.G* **G32** (2006) 73–92, [[arXiv:hep-ph/0503096](#)] [[INSPIRE](#)].
- [64] F. del Aguila and J. Aguilar-Saavedra, *Distinguishing seesaw models at LHC with multi-lepton signals*, *Nucl.Phys.* **B813** (2009) 22–90, [[arXiv:0808.2468](#)] [[INSPIRE](#)].
- [65] A. Akeroyd, C.-W. Chiang, and N. Gaur, *Leptonic signatures of doubly charged Higgs boson production at the LHC*, *JHEP* **1011** (2010) 005, [[arXiv:1009.2780](#)] [[INSPIRE](#)].
- [66] B. Dion, T. Gregoire, D. London, L. Marleau, and H. Nadeau, *Bilepton production at hadron colliders*, *Phys.Rev.* **D59** (1999) 075006, [[arXiv:hep-ph/9810534](#)] [[INSPIRE](#)].

- [67] F. Cuyper and S. Davidson, *Bileptons: Present limits and future prospects*, *Eur.Phys.J.* **C2** (1998) 503–528, [[arXiv:hep-ph/9609487](#)] [[InSPIRE](#)].
- [68] F. del Aguila, J. Aguilar-Saavedra, and J. de Blas, *Trilepton signals: the golden channel for seesaw searches at LHC*, *Acta Phys.Polon.* **B40** (2009) 2901–2911, [[arXiv:0910.2720](#)] [[InSPIRE](#)].
- [69] F. del Aguila, J. A. Aguilar-Saavedra, and J. de Blas, *New neutrino interactions at large colliders*, *PoS ICHEP2010* (2010) 296, [[arXiv:1012.1327](#)] [[InSPIRE](#)].
- [70] P. Nath, B. D. Nelson, H. Davoudiasl, B. Dutta, D. Feldman, *et al.*, *The Hunt for New Physics at the Large Hadron Collider*, *Nucl.Phys.Proc.Suppl.* **200-202** (2010) 185–417, [[arXiv:1001.2693](#)] [[InSPIRE](#)].
- [71] **CMS Collaboration**, *Inclusive search for doubly charged higgs in leptonic final states at $\sqrt{s} = 7$ TeV*. CMS-PAS-HIG-11-007, 2011. <http://cdsweb.cern.ch/record/1369542>.
- [72] **DELPHI Collaboration** Collaboration, J. Abdallah *et al.*, *Search for doubly charged Higgs bosons at LEP-2*, *Phys.Lett.* **B552** (2003) 127–137, [[arXiv:hep-ex/0303026](#)] [[InSPIRE](#)].
- [73] **OPAL Collaboration** Collaboration, G. Abbiendi *et al.*, *Search for doubly charged Higgs bosons with the OPAL detector at LEP*, *Phys.Lett.* **B526** (2002) 221–232, [[arXiv:hep-ex/0111059](#)] [[InSPIRE](#)].
- [74] **L3 Collaboration** Collaboration, P. Achard *et al.*, *Search for doubly charged Higgs bosons at LEP*, *Phys.Lett.* **B576** (2003) 18–28, [[arXiv:hep-ex/0309076](#)] [[InSPIRE](#)].
- [75] **OPAL Collaboration** Collaboration, G. Abbiendi *et al.*, *Search for the single production of doubly charged Higgs bosons and constraints on their couplings from Bhabha scattering*, *Phys.Lett.* **B577** (2003) 93–108, [[arXiv:hep-ex/0308052](#)] [[InSPIRE](#)].
- [76] **DO Collaboration** Collaboration, V. Abazov *et al.*, *Search for doubly-charged Higgs boson pair production in the decay to $\mu^+\mu^+\mu^-\mu^-$ in $p\bar{p}$ collisions at $\sqrt{s} = 1.96$ TeV*, *Phys.Rev.Lett.* **93** (2004) 141801, [[arXiv:hep-ex/0404015](#)] [[InSPIRE](#)].
- [77] **CDF Collaboration** Collaboration, D. Acosta *et al.*, *Search for doubly-charged Higgs bosons decaying to dileptons in $p\bar{p}$ collisions at $\sqrt{s} = 1.96$ TeV*, *Phys.Rev.Lett.* **93** (2004) 221802, [[arXiv:hep-ex/0406073](#)] [[InSPIRE](#)].
- [78] **CDF Collaboration** Collaboration, D. Acosta *et al.*, *Search for long-lived doubly-charged Higgs bosons in $p\bar{p}$ collisions at $\sqrt{s} = 1.96$ TeV*, *Phys.Rev.Lett.* **95** (2005) 071801, [[arXiv:hep-ex/0503004](#)] [[InSPIRE](#)].

- [79] A. Melfo, M. Nemevsek, F. Nesti, G. Senjanovic, and Y. Zhang, *Type II Seesaw at LHC: The Roadmap*, [[arXiv:1108.4416](#)] [[InSPIRE](#)].
- [80] V. Tello, M. Nemevsek, F. Nesti, G. Senjanovic, and F. Vissani, *Left-Right Symmetry: from LHC to Neutrinoless Double Beta Decay*, *Phys.Rev.Lett.* **106** (2011) 151801, [[arXiv:1011.3522](#)] [[InSPIRE](#)].
- [81] P. H. Frampton, S. L. Glashow, and D. Marfatia, *Zeroes of the neutrino mass matrix*, *Phys.Lett.* **B536** (2002) 79–82, [[arXiv:hep-ph/0201008](#)] [[InSPIRE](#)].
- [82] Z.-z. Xing, *Texture zeros and Majorana phases of the neutrino mass matrix*, *Phys.Lett.* **B530** (2002) 159–166, [[arXiv:hep-ph/0201151](#)] [[InSPIRE](#)].
- [83] H. Fritzsch, Z.-z. Xing, and S. Zhou, *Two-zero Textures of the Majorana Neutrino Mass Matrix and Current Experimental Tests*, *JHEP* **1109** (2011) 083, [[arXiv:1108.4534](#)] [[InSPIRE](#)].
- [84] B. Brahmachari and E. Ma, *Neutrinoless double beta decay with negligible neutrino mass*, *Phys.Lett.* **B536** (2002) 259–262, [[arXiv:hep-ph/0202262](#)] [[InSPIRE](#)].
- [85] **ATLAS** Collaboration, *Combined Standard Model Higgs boson searches with up to 2.3 fb⁻¹ of pp collisions at $\sqrt{s} = 7$ TeV at the LHC*. ATLAS-CONF-2011-157, 2011. <http://cdsweb.cern.ch/record/1399599>.
- [86] **CMS** Collaboration, *Combined Standard Model Higgs boson searches with up to 2.3 inverse femtobarns of pp collision data at $\sqrt{s} = 7$ TeV at the LHC*. CMS-PAS-HIG-11-023, 2011. <http://cdsweb.cern.ch/record/1399607>.
- [87] F. del Aguila and J. de Blas, *Electroweak constraints on new physics*, [[arXiv:1105.6103](#)] [[InSPIRE](#)].
- [88] F. del Aguila, J. Aguilar-Saavedra, J. . de Blas, and M. Perez-Victoria, *Electroweak constraints on see-saw messengers and their implications for LHC*, [[arXiv:0806.1023](#)] [[InSPIRE](#)].
- [89] M. Einhorn, D. Jones, and M. Veltman, *Heavy Particles and the rho Parameter in the Standard Model*, *Nucl.Phys.* **B191** (1981) 146 [[InSPIRE](#)].
- [90] M. Golden, *An upper limit on the masses of the charged Higgs bosons in the Gelmini-Roncadelli model*, *Phys.Lett.* **B169** (1986) 248 [[InSPIRE](#)].